



DEVELOPMENT OF BEM FOR CERAMIC COMPOSITES

**INTERIM STATUS REPORT
March 1988 - December 1988**

Grant No. NAG3-888

Prepared by:

**P.K. Banerjee
G.F. Dargush
D.P. Henry**

**Department of Civil Engineering
State University of New York at Buffalo**

Prepared for:

**National Aeronautics and Space Administration
Lewis Research Center
21000 Brookpark Road
Cleveland, Ohio 44135**

TABLE OF CONTENTS

	Page
1. INTRODUCTION	1
2. REVIEW OF EXISTING APPROACHES	4
3. BOUNDARY ELEMENT FORMULATION FOR CERAMIC COMPOSITES	9
3.1 Introduction	9
3.2 Boundary Integral Equations	9
3.3 Numerical Implementation	12
3.3.1 Discretization	12
3.3.2 Numerical Integration	14
3.3.3 Assembly of Equations for Composite Inserts	15
3.4 Interior Quantities	17
4. COMPUTER PROGRAM DEVELOPMENT	19
4.1 Introduction	19
4.2 Program Structure	19
4.3 Program Input	20
4.4 Surface Integration Calculation	23
4.5 System Matrix Assembly	25
4.6 System Equation Solution	28
5. PROGRAM DATA INPUT AND RESULTS	29
5.1 Input Description	29
5.2 Sample Input	36
5.3 Output Description	39
5.4 Sample Output	40
6. EXAMPLES OF COMPOSITE INSERT ANALYSIS	45
6.1 Introduction	45
6.2 Cube with a Single Insert	45
6.3 Lateral Behavior of a Cube with Multiple Inserts	47
6.4 Thick Cylinder with Circumferential Insert Supports	48
6.5 Cube with Multiple Inserts at Random Orientations	49
6.6 Beam with Insert Reinforcements in Bending	50
6.7 Laminate-Fiber Composite	51
7. SUMMARY OF CURRENT ACHIEVEMENT	65
8. FUTURE DEVELOPMENT	67
REFERENCES	71

1. INTRODUCTION

Although from a historical point of view, composite materials have found practical use for centuries, during the past two decades there has been a tremendous increase in the use of composite materials in engineering applications, particularly in aerospace engineering. One of the biggest attractions of these materials is that one is able to design and manufacture such materials to sustain a specific type of loading in a most efficient manner. If properly produced, composites can often achieve a combination of properties that are far superior to the properties of the individual constituents acting independently.

It is well known that gas turbine engine structures, particularly those components directly in the hot gas flow path, are subjected to extremely severe thermal and mechanical loading that can often lead to creep enhanced distortion, cracking and low cycle fatigue. As the demand for more efficient propulsion system rises so does the thermal and mechanical loading. It is unlikely that the current generations of metal alloys would be suitable candidates for structural components in the future generations of efficient propulsion systems. Ceramic components are often thought to be ideal as far as their thermal durability is concerned. Unfortunately, ceramics do not have adequate tensile strength to sustain a high level of mechanical loading. In recent years there has been significant effort in the attempt to incorporate fibrous inclusions within a ceramic matrix to develop a class of new materials (ceramic composites) for advanced engineering applications.

The mechanical behavior of ceramic composites under nonlinear, thermal and dynamic loading is extremely complex and can only be understood if the observed behavior is interpreted in terms of micromechanical analyses. Such analyses must take care of the complex interaction of the individual

fibers or bundles of fibers embedded in the three-dimensional ceramic matrix and must allow for increasing levels of sophistication in terms of the idealization of the fibers as well as the ceramic matrix. In addition complex interface behavior and controlled failure of the fiber must be considered.

This report details progress made during the period of March 1988 to December 1988 in a five-year program commencing in March 1988, towards the development of a boundary element code designed for the micromechanical studies of advanced ceramic composites. Additional effort has been made in generalizing the implementation to allow the program to be applicable to real problems in the aerospace industry.

The primary goal of the first year has been to develop the boundary integral formulation for a fully-bonded elastic inclusion within an elastic matrix, and to implement the formulation in a boundary element program in a sufficiently general manner as to facilitate implementation of future development for the remainder of the present program of research.

Significant progress has been achieved during the first year of the present effort. The analytic and numerical basis for the ceramic composite program has been developed. This effort included:

1. the derivation of the boundary integral formulation modified for holes and inserts,
2. the derivation of the kernel function for one-dimensional line integration of holes and inserts,
3. the implementation for the assembly and solution of inserts, and
4. the validation and verification runs using the developed computer code.

The ceramic composite formulation has been implemented in the three-dimensional boundary element computer code 'BEST3D' which was developed for NASA by Pratt and Whitney and the State University of New York at Buffalo under contract NAS3-23697. BEST3D has been adopted as the base for the ceramic composite program, so that many of the enhanced features of this general purpose boundary element code can be utilized. Some of these facilities include sophisticated numerical integration, the capability of local definition of boundary conditions, and the use of quadratic shape functions for modeling geometry and field variables on the boundary. The multi-region implementation permits a body to be modeled in substructural parts; thus dramatically reducing the cost of the analysis. Furthermore, it allows a body consisting of regions of different ceramic matrices and inserts to be studied.

In the next section, the existing approaches for the study of the micromechanical behavior of composites are briefly reviewed. This is followed by the development of the boundary element formulation for ceramic composites in Section 3. Section 4 outlines the development of the general computer program implementation followed by the description of the program's data input and output in Section 5. Example data and results are included to demonstrate the convenience in modeling and analyzing composites using this code. In Section 6, a number of numerical examples are presented to demonstrate the power of the present implementation. This report is then concluded with a summary and plan for future development.

2. REVIEW OF EXISTING APPROACHES

A number of techniques of varying degree of sophistication are presently used to study the micromechanical behavior of composites. In essence the various micromechanical analyses recognize the inhomogeneous nature of the composite material, but generally ignore finer details of the structure of the fiber and matrix to a varying degree. Numerous approximations are made concerning the packing geometry and response fields within the body so that mathematical analyses can be performed to relate the properties and concentration of fibers and matrix to the average property of the body. A complete bibliography of these methods which are variously called 'mechanics of materials', 'self-consistent fields', 'variational methods' and 'numerical techniques' are given in Chamis and Sendekyj (1968).

Although none of the above mentioned work specifically focuses on ceramic composites (and it appears that very little is available in the current literature), the overall conclusions derived apply reasonably well to the present case.

Rational methods based on mechanics of materials have been developed over the last decade to explain and predict the behavior of composite systems in terms of their materials make-up. Some of these simple models have indeed been very effective. For example, a simple model of the fiber and resin components responding by parallel reactions to imposed thermal or mechanical loads is generally adequate to describe and predict the following longitudinal properties of unidirectional composites:

- Longitudinal modulus E_L ;
- Poisson's ratio, ν_{12} ;
- Linear thermal expansion coefficient, α_L ;
- Thermal conductivity, K_L .

Primary emphasis in the model has been given to stiffness-limited structures so that attention has been focused on the longitudinal modulus. For all practical purposes the contributions of the matrix phase to this property are often assumed negligible.

The properties perpendicular to the direction of the fibers are not so simply described nor so readily predicted. A simple model of the fiber and matrix components responding in series to imposed loads leads to conservative estimates of the properties in this direction. More comprehensive and elaborate models show that the transverse properties and shear moduli are sensitive to:

- the shape of the fibers;
- the packing geometry of the fibers;
- the variations in spacings of the fibers;
- the properties of the matrix.

Ambiguities in the theoretical models make it difficult to isolate and identify the extent to which each of these factors influences the transverse properties and shear moduli of composites: qualitatively, it is clear that the matrix dominates the behavior of these properties.

A model for compressive strength based on a failure mode of in-phase fiber buckling leads to the conclusion that the compressive strength of unidirectional composites is determined by the shear modulus of the matrix. Experimental observations can be rationalized in terms of this model if the effective shear modulus of the matrix is assumed to be less than that of the comparable bulk material. Adherence to this model further requires that the effective shear modulus of the matrix be dependent upon the system of reinforcing fibers used and/or dependent upon the degree of adhesion between the fibers and the matrix.

Current theoretical models cannot unambiguously explain or predict the tensile strength of unidirectional composites; however, examination of models for the extremes of fiber-matrix coupling leads to a qualitative identification of the critical factors that influence tensile strength:

- the statistics of the fiber strengths;
- load transfer efficiency;
- resistance of the matrix to crack propagation;
- the adhesive bond strengths between the fiber and the matrix

The direct contribution of the strength of the matrix to the tensile strength of the composite is negligible; nonetheless, an imperfect matrix can seriously detract from the realization of the full strength potential of the fibers through indirect influences involved in load-transfer efficiency or crack sensitivity.

Load-transfer efficiency and crack sensitivity appear to be diametric functions of the adhesive bond strength between the fiber and the matrix. This implies that some optimum (not necessarily a maximum) adhesive bond strength is required to establish a proper balance between load transfer efficiency and the overall strength-toughness of the composite.

It was suggested in some physiochemical models that the molecular mechanisms involved in achieving adhesion between the fiber and matrix could significantly perturb the molecular structure of the matrix; these structural perturbations may develop in an interphase region whose properties differ appreciably from the properties of bulk material. Additionally, stress diffusion from fiber to the matrix may also alter the properties of the matrix locally. Since very large surface areas are involved in the contact between the fiber and the matrix, a sufficient quantity of interphase material could be generated to influence the average

in situ properties of the matrix. Hence, it is reasonable to expect that the average properties of matrix in composites may differ from the corresponding properties of bulk material and may differ between various reinforcing fiber systems.

In conclusion, the contributions of the reinforcing fibers to the performance of composite materials are qualitatively well understood. Fiber dominated properties (i.e., the longitudinal modulus) can be adequately explained and predicted. The direct contribution of the matrix to the longitudinal modulus and tensile strength is negligible; however, secondary effects associated with the matrix can detract from the potential tensile strength of the system. Although current simple theoretical models indicate that the matrix controls the compressive strength, transverse moduli, and shear moduli of composites, this is not sufficient for the solution of boundary value problems involving nonlinear, thermal, and dynamic loading.

Comparatively little effort has been given to identify the specific roles of the matrix in the overall performance of advanced composite materials. This is largely due to the emphasis on longitudinal modulus as well as the theoretical and experimental difficulties involved in isolating the contributions of the matrix from effects due to fiber shape and packing geometry. The possibility that the properties of the matrix can differ from the properties of bulk material, as well as differ between various fiber systems, further complicates the in situ matrix.

Since the interaction of the fiber and matrix is complex, it is likely that the best technique to use to study the micromechanical behavior would be a numerical method. It is therefore not surprising that the finite element method is often used to develop the micromechanical model. Although it is perhaps the most powerful numerical method over the entire

spectrum of engineering science, it has never been fully satisfactory for problems with high stress gradient, complex interface phenomena, high thermal gradients and large variations in the stiffness within the same body. Unfortunately all of these occur within a ceramic composite assembly. Nevertheless, the use of finite element to study the micromechanics of composites is quite common, perhaps primarily due to the absence of a reasonable alternative.

3. BOUNDARY ELEMENT FORMULATION FOR CERAMIC COMPOSITES

3.1 Introduction

It is evident that for proper micromechanical analysis of ceramic composites one needs to use a numerical method that is capable of idealizing the individual fibers or individual bundles of fibers embedded within a three-dimensional ceramic matrix. The analysis must be able to take account of high stress gradients from diffusion of stress from the fiber to the ceramic matrix and allow for the interaction between the fibers through the ceramic matrix. The analysis must be sophisticated enough to deal with failure of fibers described by a series of increasingly sophisticated constitutive models. Finally, the analysis must deal with micromechanical modeling of the composite under nonlinear thermal and dynamic loading.

The boundary element method is uniquely suited for the task. BEM has proven its ability to accurately determine stress near stress concentration. All functional quantities in a BEM system are on the boundary and interface surfaces, therefore, allowing nonlinear interaction between the matrix and insert interface to be readily described by failure models. Furthermore, recent development has shown the generality and versatility of boundary element method in analyzing large two- and three-dimensional models subjected to static, dynamic and thermal loads involving materials with nonlinear behavior.

3.2 Boundary Integral Equations

The conventional boundary integral equation for displacement is the starting point for the ceramic composite formulation. The displacement for a point ξ inside the elastic composite matrix is given below

$$C_{ij}(\xi)u_i(\xi) = \int_S [G_{ij}(x, \xi)t_j(x) - F_{ij}(x, \xi)u_j(x)]dS(x)$$

$$+ \sum_{n=1}^N \int_{S^n} [G_{ij}(x, \xi) t_i(x) - F_{ij}(x, \xi) u_i(x)] dS^n(x) \quad i, j = 1, 2, 3 \quad (3.1)$$

where

G_{ij}, F_{ij} are the fundamental solutions of the governing differential equations of the ceramic matrix of infinite extent

C_{ij} are constants determined by the relative smoothness at ξ

u_i, t_i are displacements and tractions

S, S^n are surfaces of the matrix and holes (left for fiber) respectively

N is the number of fibers

The conventional boundary integral equation for displacement can also be written for each of the N insert fibers. For the displacement at a point ξ inside the m^{th} insert we can write

$$C_{ij}^m(\xi) \bar{u}_i(\xi) = \int_{S^m} [G_{ij}^m(x, \xi) \bar{t}_i(x) - F_{ij}^m(x, \xi) \bar{u}_i(x)] dS^m(x) \quad (3.2)$$

$i, j = 1, 2, 3$

G_{ij}^m, F_{ij}^m are the fundamental solutions of the m^{th} insert

C_{ij}^m are constants determined by the relative smoothness at ξ in insert m

\bar{u}_i, \bar{t}_i are displacement and tractions associated with the m^{th} insert

S^m the surface of the m^{th} insert

We next examine the interface conditions between the composite matrix and the insert. For a perfect bond the displacement of the matrix and the displacement of the inserts along the interface the interface are equal and the tractions are equal and opposite.

$$\bar{u}_j(x) = u_j(x) \quad (3.3a)$$

$$\bar{t}_j(x) = -t_j(x) \quad (3.3b)$$

For a stiff insert in which the elastic modulus is much greater than the modulus of the composite matrix, the Poisson ratio of the insert can be assumed equal to that of the matrix with little error. Therefore, upon consideration of the surface normals at the interface and examination of the F_{ij} kernels, we can write the following relation for the m^{th} insert

$$F_{ij}^m(x, \xi) = -F_{ij}(x, \xi) \quad (3.3c)$$

Substitution of equations (3.3) into equation (3.2) yields the following modified boundary integral equation for insert m .

$$\bar{C}_{ij}^m(\xi)u_i(\xi) = \int_{S^m} [-G_{ij}^m(x, \xi)t_i(\xi) + F_{ij}(x, \xi)u_i(x)]dS^m(x) \quad (3.4)$$

Finally adding N insert equations (3.4) to equation (3.1) and cancelling terms, yields the modified boundary integral equation for the composite matrix

$$\begin{aligned} \bar{C}_{ij}(\xi)u_i(\xi) &= \int_S [G_{ij}(x, \xi)t_i(x) - F_{ij}(x, \xi)u_i(x)]dS(x) \\ &+ \sum_{n=1}^N \int_{S^n} [\bar{G}_{ij}(x, \xi)t_i(x)]dS^n(x) \end{aligned} \quad (3.5)$$

where

$$\bar{G}_{ij}(x, \xi) = G_{ij}(x, \xi) - G_{ij}^m(x, \xi)$$

\bar{C}_{ij} constants dependent on the geometry at ξ

3.3 Numerical Implementation

3.3.1 Discretization

The integral representations of the previous section are exact statements of the ceramic composite problem, however, approximations such as finite discretization and numerical integration are necessary in order to obtain a solution to non-trivial problems. The goal of the numerical implementation of the present formulation is to obtain the most accurate and efficient implementation possible.

The first step in this process is the conversion of the two-dimensional kernel integral over the surface of the hole and insert into a line integral. By performing an analytical integration in the circumferential direction on the surface of the hole (or insert) a considerable amount of computational time can be saved in the numerical integration. In this process the holes and inserts are assumed to be circular and a circumferential variation of $a_0 + a_1 \cos\theta + a_2 \sin\theta$ is assumed in the displacements and tractions on the surface of the holes and inserts. Furthermore, tensor transformations on the kernels are necessary for inserts oriented at oblique angles with respect to the global axes. The resulting kernels, which contain a large family of elliptical integrals, are long and formidable. The complexity of these kernels prohibits their presentation in a tidy manner, and therefore, they have not been presented in this report.

Once the analytical integration is complete, the inserts are discretized in their axial direction using linear or quadratic shape functions. In discretized form, equation (3.4) can be written for a single insert as

$$\begin{aligned}
\bar{C}_{ij}^m(\xi)u_i(\xi) &= - \sum_{p=1}^P \left[\int_{S^p} G_{ij}^m(x, \xi) N^\gamma(\eta) dS^p \right] t_i^\gamma \\
&+ \sum_{p=1}^P \left[\int_{S^p} F_{ij}^m(x, \xi) N^\gamma(\eta) dS^p \right] u_i^\gamma
\end{aligned} \tag{3.6}$$

where P is the number of line elements, and $N^\gamma(\eta)$ represents the shape function across the line element. Summation over γ is implied.

In a similar manner, equation (3.5) can be discretized using one- and two-dimensional shape functions in the following manner.

$$\begin{aligned}
\bar{C}_{ij}(\xi)u_i(\xi) &= \sum_{q=1}^Q \left[\int_{S^q} G_{ij}(x, \xi) M^\beta(\eta_1, \eta_2) dS^q \right] t_i^\beta \\
&- \sum_{q=1}^Q \left[\int_{S^q} F_{ij}(x, \xi) M^\beta(\eta_1, \eta_2) dS^q \right] u_i^\beta \\
&+ \sum_{p=1}^P \left[\int_{S^p} \bar{G}_{ij}(x, \xi) N^\gamma(\eta) dS^p \right] t_i^\gamma
\end{aligned} \tag{3.7}$$

where Q is the number of surface elements on the outer surface of the composite matrix of the region, and $M^\beta(\eta_1, \eta_2)$ represents the two-dimensional shape function. Summation over γ and β is implied.

Note that the same number of nodes, and consequently shape functions, are not necessarily used to describe both the geometric and functional variations. Specifically, in the present work, the geometry is exclusively defined by quadratic shape functions. On the other hand, the variation of the primary quantities can be described, within an element, by either

quadratic or linear shape functions. (The introduction of linear variations provides computationally advantageous in some instances.)

3.3.2 Numerical Integration

The complexity of the integral in the discretize equation necessitates the use of numerical integration for their evaluation. The steps in the integration process for a given element is outlined below:

1. Using appropriate Jacobian transformations, the curvilinear line elements and surface elements are mapped onto a unit line and planar unit cells, respectively.

2. Depending on the proximity between the field point (ξ) and the element under consideration, there may be element subdivision and additional mapping for improved accuracy.

3. Gaussian quadrature formulas are employed for the evaluation of the discretized integral over each element (or sub-element). These formulas approximate the integral as a sum of weighted function values at designated points. The error in the approximation is dependent on the order of the (Gauss) points employed in the formula. To minimize error while at the same time maintaining computational efficiency, optimization schemes are used to choose the best number of points for a particular field point and element (Watson, 1979).

4. When the field point coincides with a node of the element being integrated, the integration becomes singular. In this case, the value of the coefficients of the F_{ij} kernel corresponding to the singular node cannot be calculated accurately by numerical integration. Instead, after the integration of all elements is complete, this value is determined so as to satisfy a rigid body displacement of the body (Banerjee and Butterfield, 1981).

3.3.3 Assembly of Equations for Composite Inserts

After the derivation of the modified boundary integral equations and the analytical circumferential integration of the kernel functions, the next critical step in the formulation is the assembly of the inserts into the system equations. Here, efficiency is of utmost importance. The approach to writing an efficient algorithm is to keep the number of system equations to a minimum by eliminating all unnecessary unknowns from the system. The strategy used is to retain in the system only traction variables on the matrix/insert interface. This is in contrast to a general multi-region problem where both displacement and tractions are retained on an interface. The elimination of the displacements on the interface is achieved through a backsubstitution of the insert equations into the system equations which are made up exclusively from equations written for the composite matrix (on the outer surface and on the surface of the holes). The procedure is described below.

Equation (3.7) is used to generate a system of equations for nodes on the outer surface of the matrix and for nodes on the surface of the holes containing the inserts. Written in matrix we have

$$\text{On Matrix Surface:} \quad Gt - Fu + \bar{G}t^H = 0 \quad (3.8a)$$

$$\text{On Hole for Insert:} \quad Gt - Fu + \bar{G}t^H = Iu^H \quad (3.8b)$$

where

t and u are traction and displacement vectors on the outer surface of the composite matrix

t^H and u^H are traction and displacement vectors on the hole

I is the identity matrix

Our goal is to eliminate u^H from the system. To this end, equation (3.6) is written for each node on an insert, collocating slightly outside the

insert [where $C_{ij}^n = 0$], we obtain

$$Fu^H = Gt^H \quad (3.9)$$

Post multiplying equation (3.8b) by the F matrix in equation (3.9) yields

$$FGt = FFu + \bar{FG}t^H = Fu^H \quad (3.10)$$

Equation (3.9) can now be set equal to equation (3.10) and the final form of the system is derived.

$$\begin{aligned} \text{On Matrix:} \quad & Gt - Fu + \bar{G}t^H = 0 \\ \text{On Hole:} \quad & FGt - FFu + (FG - G)t^H = 0 \end{aligned} \quad (3.11)$$

At every point on the outer surface, either the traction or the displacement is specified and on the surface of the hole only the tractions are retained. Therefore, the number of equations in the system are equal to the final number of unknowns, and hence, the system may be solved. Thereafter, equation (3.8b) is used to determine the displacement on the matrix/insert interface.

It should be noted that since the displacement about a particular hole is present only in the insert equation corresponding to that hole, backsubstitution can be performed one insert at a time in a more efficient manner than backsubstitution of all inserts at once. Further note that nowhere in the assembly process is a matrix inversion necessary. This efficient assembly process was made possible due to the unique formulation of the modified boundary integral equations developed earlier in this section.

When the composite matrix is divided into a multi-region model, the above insert assembly is performed for each region independently. Thereafter, equilibrium and compatibility conditions are invoked at common

interfaces of the substructured matrix composite. After collecting together the known and unknown boundary quantities, the final system can be expressed as

$$A^b x = B^b y \quad (3.12)$$

where

x is the vector of unknown variables at boundary and interface nodes,

y is the vector of known variables, and

A^b, B^b are the coefficient matrices

Standard numerical procedures can be used to solve the unknowns in equation (3.12). Details are described in the computer development section.

3.4 Interior Quantities

Once all the displacements and tractions are known on the matrix outersurface and on the matrix/insert interface, interior quantities of displacement, stress and strain can be determined at any point in the composite matrix or in the insert. For displacement either the conventional boundary displacement integral equation (3.1) or (3.2) can be employed or alternatively the modified equations (3.3) or (3.5) can be used.

Equations for strains can be derived from the forementioned displacement equations and the strain-displacement relations. Thereafter, equations for stress are obtained by substituting the resulting strain equations into Hooke's law.

The resulting equations, however, are not only invalid on the surface, but also difficult to evaluate numerically at points close to it. For points on the surface, the stresses can be calculated by constructing a

local Cartesian coordinate system with the axes 1 and 2 directed along the tangential directions and the axis 3 in the direction of the outward normal. The stresses $\bar{\sigma}_{ij}$ referred to these local axes (indicated by overbars) are then given by:

$$\bar{\sigma}_{11} = \frac{\nu}{1-\nu} \bar{t}_3 + \frac{E\nu}{1-\nu^2} (\bar{\epsilon}_{11} + \bar{\epsilon}_{22}) + \frac{E}{1+\nu} \bar{\epsilon}_{11}$$

$$\bar{\sigma}_{12} = \bar{\sigma}_{21} = \frac{E}{2(1+\nu)} \bar{\epsilon}_{12}$$

$$\bar{\sigma}_{22} = \frac{\nu}{1-\nu} \bar{t}_3 + \frac{E\nu}{1-\nu^2} (\bar{\epsilon}_{11} + \bar{\epsilon}_{22}) + \frac{E}{1+\nu} \bar{\epsilon}_{22}$$

(3.13)

$$\bar{\sigma}_{33} = \bar{t}_3$$

$$\bar{\sigma}_{32} = \bar{\sigma}_{23} = \bar{t}_2$$

$$\bar{\sigma}_{31} = \bar{\sigma}_{13} = \bar{t}_1$$

where E is the Young's modulus, $\bar{\epsilon}_{ij}$ defines the components of the strains in the local axes system and \bar{t}_i are the traction on the boundary. This method of evaluating the stresses on the surface was originally devised by (Rizzo and Shippy, 1968).

4. COMPUTER PROGRAM DEVELOPMENT

4.1 Introduction

The goal of the computer program developed for ceramic composites is the accurate and efficient implementation of the formulation described in Section 3. Of equal importance is the degree of generality required in the definition of component geometry, loading and material properties. This is necessary if the program is to be applicable to real problems in the aerospace industry.

For this reason the ceramic composite formulation has been implemented in the three-dimensional boundary element computer code 'BEST3D' (Boundary Element Stress Technology - Three-dimensional) which was developed for NASA by Pratt and Whitney and SUNY/Buffalo under contract NAS3-23697. Since its development, BEST3D has proven itself to be a highly accurate and numerically efficient boundary element program.

The development of the computer program 'Composite-BEST' is discussed in the following sections.

4.2 Program Structure

Composite-BEST is designed to be a fully general ceramic composite analysis system employing the boundary element method. The program is written using standard FORTRAN 77. Development has been carried out at SUNY/Buffalo on an HP9000 minicomputer system. The required code and workspace fit in core without requirement for overlays. The nature of the method is such that, for any realistic problem, not all required data can reside simultaneously in core. For this reason extensive use is made of both sequential and direct access scratch files.

The program first executes an input segment. After the input has been processed, the surface integrals are calculated and assembled into the set

of system equations using specified boundary conditions, followed by the insert assembly and the inclusion of the insert equations into the general system. The system matrix is then decomposed and saved on disk, followed by the calculation of the solution vector. The full displacement and traction solution on each boundary element and insert element is then reconstructed from the solution vector. In a time dependent problem the process of constructing the load vector for the system equations is repeated at each time step, but the integration, formation and decomposition of the system matrix are done only once.

Various aspects of the computer program are discussed below.

4.3 Program Input

The input for Composite-BEST is free field. Meaningful keywords are used to identify data types and to name particular data sets. The input is divided into five types:

1. Case Control Cards

The case control cards define global characteristics of the problem. In addition to the problem title, the times for multiple time steps are defined. The reading or writing of restart data is also defined at this point. The restart facility allows one to change the arrangements of fibers without recalculating the various coefficients.

2. Material Property Definition

The material property input allows the definition of material properties for a variety of materials. The Young's modulus can be prescribed in tabular form for a user-defined set of temperatures. Temperature independent values of Poisson's ratio are also defined.

3. Geometry Input

Geometry input is defined one GMR (generic modeling region, or subregion) at a time. To initiate the input, a tag is provided to identify the GMR, a material name and reference temperature are defined to allow initialization of material properties.

The next block of geometry input consists of the Cartesian coordinates of the user input points for the outer surface geometry definition of the composite matrix, together with identifiers (normally positive integers) for these geometric nodes.

Following the definition of an initial set of nodal points, the surface connectivity of the outer surface of the composite matrix is defined through the input of one or more named surfaces. Each surface is made up of a number of elements, with each element defined in terms of several geometric nodes. Three sided elements, defined using six rather than eight geometric nodes, are used for mesh transition purposes. The terms quadrilateral and triangle are normally used to refer to the eight and six noded elements, although the real geometry represented is, in general, a nonplanar surface patch. Seven and nine noded elements are made available by adding a central node to the six or eight noded elements.

Over each element the variation of displacement and traction can be defined using either the linear or quadratic shape functions. Linear and quadratic elements can share a common side, which is then constrained to have linear displacement and traction variation.

Finally an option is available to allow quadratic functional variation (8 or 6 nodes) to be used in conjunction with linear geometry (4 or 3 nodes). In this case the program generates the additional nodes automatically at mid-point of the sides. The characteristics of the various element types are summarized below.

Surface Element Type	Geometry Nodes	Displacement/Traction Nodes
Linear Quadrilateral	8 or 9	4
Linear Triangle	6 or 7	3
Quadratic Quadrilateral	8 or 9	8 or 9
Quadratic Triangle	6 or 7	6 or 7
Quadratic Quadrilateral	4	8
Quadratic Triangle	3	6

Following the definition for the composite matrix outer surface, the embedded inserts are then defined. These are defined as curvilinear line elements with a prescribed radius of cross-section. The inserts are generally straight, however as noted, curved inserts are also allowed. The user first defines the nodal coordinates of the centerline of the insert. Thereafter, the radius and the insert connectivity is defined. Linear and quadratic elements are available for both geometry and functional variation, however, quadratic functional variation over linear geometry is not presently available. The various options for the insert elements are summarized below.

Insert Element Type	Geometry Nodes	Displacement/Traction Nodes
Linear-Linear	2	2
Quadratic-Linear	3	2
Quadratic-Quadratic	3	3

Note only the surface of the insert needs to be defined, i.e., the hole in the composite matrix which encompasses the insert does not have to be explicitly defined.

4. Interface Conditions

The interface input describes the connection of surfaces or elements of one composite matrix region to another. Interfaces between the composite matrix and inserts do not have to be defined. Special types of interface conditions which are available presently include fully-bonded and

sliding contact between two GMRs, and springs to other regions. In the current implementation, fully-bonded connections between the insert and matrix has been assumed. This will be relaxed in later work.

5. Boundary Condition Input

The final input section provides for the definition of boundary conditions, as functions of both position and time. Data can be input for an entire surface, or for a subset (elements or nodes) of a surface. Input can be in global coordinates, or can define rollers or pressure in the local coordinate system. Input simplifications are available for the frequently occurring cases of boundary data which is constant with respect to space and/or time variation. Each boundary condition set can be defined at a different set of times.

4.4 Surface Integral Calculation

Following the processing of the input data, the surface integrals occurring in equations 3.6 and 3.7 are evaluated numerically. This is the most time consuming portion of the analyses. In Composite-BEST the results of these integrations are stored as they are calculated, rather than being assembled into the final equation system immediately. Although this is somewhat more costly in terms of storage and CPU (central processing unit) time, it has led to much greater clarity in the writing of Composite-BEST. In addition, it provides much greater flexibility in the implementation of various restart and boundary condition options.

The calculations proceed first by GMR (generic modeling region), then by source point (the equation being constructed) and finally by surface element and insert element. The results for each source point element pair are written to disk. All of the calculations are carried out and stored in the global (Cartesian) coordinate system.

The integration of the BEM equations is the most complex part of the code. In this process either singular or nonsingular integrals can be encountered. The integrals are singular if the source point for the equations being constructed lies on the element being integrated. Otherwise, the integrals are nonsingular, although numerical evaluation is still difficult if the source point and the element being integrated are close together.

In both the singular and nonsingular cases Gaussian integration is used. The basic technique is developed in Banerjee and Butterfield, 1981. In the nonsingular case an approximate error estimate for the integral was developed based on the work of Stroud and Secrest (1966). This allows the determination of element subdivisions and orders of Gaussian integration which will retain a consistent level of error throughout the structure. Numerical tests have shown that the use of 3, 4, and 5 point Gauss rules provide the best combination of accuracy and efficiency. In the present code the 4 point rule is used for nonsingular integration, and error is controlled through element subdivision. The origin of the element subdivision is taken to be the closest point to the source point on the element being integrated.

If the source point is very close to the element being integrated, the use of a uniform subdivision of the element can lead to excessive computing time. This frequently happens in the case of aerospace structures, due either to mesh transitions or to the analysis of thin walled structures. In order to improve efficiency, while retaining accuracy, a graded element subdivision was employed. Based on one-dimensional tests, it was found that the subelement divisions could be allowed to grow geometrically away from the origin of the element subdivision. Numerical tests on a complex three-dimensional problem have shown that a mesh expansion factor as high

as 4.0 can be employed without significant degradation of accuracy.

In each case of singular integration (source point on the elements being integrated) the element is first divided into subelements. The integration over each subelement is carried out using a Jacobian transformation in mapping. This coordinate transformation produces nonsingular behavior in all except one of the required integrals. Normal Gauss rules can then be employed. The remaining integral (that of the traction kernel F_{ij} times the isoparametric shape function which is 1.0 at the source point) is still singular, and cannot be numerically evaluated with reasonable efficiency and accuracy. Its calculation is carried out indirectly, using the fact that the stresses due to a rigid body translation are zero (Lachat and Watson, 1976). It has been found that subdivision in the circumferential direction of a two-dimensional surface element is required to preserve accuracy in the singular integration of the outer surface. A maximum included angle of 15 degrees is used. Subdivision in the radial direction has not been required.

The integrals required for calculation of displacement and stress at interior or surface points are of the same type as those involved in the generation of the system equations, except that only nonsingular integrals are involved. If the source point involved is located on the surface of the body, then numerical integration is not required. Instead, the required quantities are calculated using the displacements and tractions on the element (or elements) containing the source point, as discussed in Section 3.4.

4.5 System Matrix Assembly

The first step in the assembly process is the reduction of the rectangular matrix of F integrals to a square matrix. This matrix is the

prototype of the system matrix. The columns of this matrix are transformed or replaced, as required by the boundary conditions, as the assembly process proceeds.

The next step in the process is the incorporation of the insert equations in the system. As was described in detail in Section 3.3.3, the insert assembly consists of an insert by insert matrix multiplication and backsubstitution. The backsubstitution minimizes the number of equations required in the system since the displacement about the insert is eliminated from the system and only tractions are retained.

A key problem in the entire process is the proper definition of appropriate coordinate systems, on a nodal basis. This is a problem common to any direct boundary element method which treats structures with nonsmooth surfaces. It arises because the tractions at a point are not uniquely determined unless the normal direction to the surface varies continuously at the point in question.

The original surface integral calculations are all done in global coordinates. If a displacement boundary condition is specified at a given node, in global coordinates, then no new coordinate system definition is required. It is only necessary to keep track of the subset of elements, containing the given node, on which the fixed displacement is to be reacted. However, if a displacement is specified in a nonglobal direction at a given node, then a new nodal coordinate system must be defined and, potentially, updated as further boundary conditions are processed. The associated nonzero reactions must then be expressed in the new coordinate system.

Following this preparatory work, the final assembly of the system equations is carried out. It is performed in three major steps:

1. Transformation of the columns of the matrices to appropriate local

coordinate systems and incorporation of any boundary conditions involving springs.

2. Incorporation of compatibility and equilibrium conditions on interfaces between GMRs. On interfaces between two composite regions either a completely bonded condition (full displacement compatibility) or a sliding condition (only normal displacement compatibility) is available. At the interface between the insert and matrix a fully bonded connection has been assumed which will be relaxed later.
3. Application of specified displacements and tractions.

Two particular features of the equation assembly deserve special comment. First, in multi-GMR problems the system matrix is not full. Rather, it can be thought of as consisting of an $N \times N$ array of submatrices, each of which is either fully populated or completely zero. Only the nonzero portions of the system equations are preserved during system matrix assembly. In order to improve the numerical conditioning of the system matrix for the solution process, the columns are reordered to number variable lying on the same interface, but belonging to two different GMRs, as close together as possible. The rows of the system matrix are placed in the same order as the columns.

Second, rather than simply assembling an explicit load vector at each time point in the solution process, load vector coefficient matrices are assembled and stored. These allow the updating of the load vector at any required time point simply by interpolating the time dependent boundary conditions and performing a matrix multiplication. A similar process is used in the calculation of interior and boundary stresses.

4.6 System Equation Solution

The solver employed in Composite-BEST operates at the submatrix level, using software from the LINPACK package (Dongarra, 1979) to carry out all operations on submatrices. The system matrix is stored, by submatrices, on a direct access file. The decomposition process is a Gaussian reduction to upper triangular (submatrix) form. The row operations required during the decomposition are stored in the space originally occupied by the lower triangle of the system matrix. Pivoting of rows within diagonal submatrices is permitted.

The calculation of the solution vector is carried out by a separate subroutine, using the decomposed form of the system matrix from the direct access file. The process of repeated solution, required for problems with multi-time steps, is highly efficient.

5. PROGRAM DATA INPUT AND RESULTS

5.1 Input Description

The input to Composite-BEST is presently divided into five sections as follows:

1. Case control (**CASE control)
2. Material properties (**MATERIAL property)
3. Generic modeling regions (**GMRegion)
4. Interfaces (**INTERface)
5. Boundary condition sets (**BCSET)

A detailed description of each of these sections is provided in the following paragraphs. The interface sections are optional; the other sections must be input at least once.

Input quantities may be either alphanumeric or numeric (integer, floating point, E, or D format) as specified and may be up to 16 characters. Individual entries on a card (both keyword and input) must be separated by at least one blank space. Input for certain keywords (as noted) may be continued onto more than one card by repeating the keyword on the new card(s).

Keywords may be input as shown; minimum input is the the CAPITALIZED characters. Those keywords which are underscored must always be input. Keywords shown below are indented to indicate groups of cards to be input together. However, it is not necessary to indent in this manner.

The current program limits include:

- 20 time points
- 15 generic modeling regions
- 600 elements (300 elements in problems having interior points)
- 2500 nodes (560 nodes per region)

- 100 inserts per generic modeling region
- 500 inserts per problem
- 1200 source points (600 source points in problems having interior points)
- 302 source points per region in a local coordinate system
- 99 interface element pairs (total)
- 350 interface node pairs (total)
- 60 boundary condition sets with springs
- maximum element number of 9999
- maximum node number of 9999
- maximum of 24 entries per input card

1. Case Control Input

<u>Keyword</u>	<u>Type of Input</u>	<u>Input</u>
** <u>CASE</u> control		
<u>TITLE</u>	Alphanumeric	Case title
REStart	Alphanumeric	READ or WRITE
<u>TIMES</u>	Numeric	Output time value(s)

The analysis is assumed to be static, constant temperature, elastic, and time independent unless the appropriate optional keyword is input. The optional keywords need be included only if a particular option is to be turned on.

The case title should have a maximum of 72 characters.

Input on the TIMES card may be continued on more than one card

2. Material Property Input

The material property input section must be repeated for each separate material.

<u>Keyword</u>	Type of <u>Input</u>	<u>Input</u>
**MATER ial property		
<u>ID</u>	Alphanumeric	Material name
<u>TEMP</u> erature	Numeric	Temperature value(s)
<u>EMOD</u> ulus	Numeric	Young's modulus value(s)
<u>POISS</u> on	Numeric	Poisson's ratio value

The Young's modulus must be input in the same order as the temperature values.

Input on the TEMPERATURE and EMODULUS cards may be continued on more than one card.

NOTE: The elastic modulus of the inserts are defined in the GMR input. The Poisson Ratio for inserts is taken to be the same as the Poisson Ratio of the Composite matrix.

3. Generic Modeling Region Input

The generic modeling region section must be repeated for each region.

<u>Keyword</u>	Type of <u>Input</u>	<u>Input</u>
**GMR		
<u>ID</u>	Alphanumeric	Region name
<u>MAT</u>	Alphanumeric	Material name
<u>TREF</u> erence	Numeric	Reference temperature value
<u>POINT</u> s	Numeric	Node number, coordinate values (x,y,z)
<u>SURF</u> ace	Alphanumeric	Surface name, (reference surface name)
<u>TYPE</u>	Alphanumeric	LINE or QUAD

<u>ELEM</u> ents	Numeric	Element number, node numbers
<u>NOR</u> Mal	Alphanumeric	Element number, + or -
<u>INS</u> ert	Numeric	Elastic modulus of insert
<u>POIN</u> ts	Numeric	Node number, coordinate value (x,y,z)
<u>TY</u> PE	Alphanumeric	LINEar or QUAD
<u>ELEM</u> ent	Numeric	Element number, radius of insert element, node numbers
<u>INT</u> erior	Alphanumeric	
<u>POIN</u> ts	Numeric	Point number, coordinate values (x,y,z) for interior sampling points

The SURFace input may be either of two forms:

- a TYPE card and an ELEMents card to define element connectivity

The TYPE designation in SURFace input specifies the traction or displacement variation on the element. A surface may contain only one TYPE card. Therefore, if mixed variation is required in a region, two surfaces must be defined.

Surface elements must have either 6 or 7 (triangles) or 8 or 9 (quadrilaterals) nodes. Element numbering is consecutive around the boundary.

Insert elements must have either 2 (linear) or 3 (quadratic) nodes. Nodes referenced in element connectivity must be explicitly defined under 'insert' POINT card and the points should not intersect the outer boundary or other insert elements.

The sign associated with the defining element on the NORMal card should be plus (+) if the element is numbered in a counterclockwise

direction as seen from the outside of the model or minus (-) if it is numbered in a clockwise direction. Disjoint boundaries must have multiple element/sign pairs on the NORMAL card.

The points which are input in the INTERIOR input are treated as "interior" points. These points may be either nodal points, other surface points, or true interior points.

4. Interface Input

The interface input describes the connection of surfaces (or elements or points) of one composite matrix region to another. Interfaces between the composite matrix and inserts do not have to be defined.

The interface section must be repeated for each interface.

<u>Keyword</u>	<u>Type of Input</u>	<u>Input</u>
**INTERface		
GMR	Alphanumeric	Region name of first region
SURFace	Alphanumeric	Surface name in first region
ELEMents	Numeric	Element number(s) in first region
POINTs	Numeric	Node number(s) in first region
GMR	Alphanumeric	Region name of second region
SURFace	Alphanumeric	Surface name in second region
ELEMents	Numeric	Element number(s) in second region
POINTs	Numeric	Element number(s) in second region
SLIDing		

The interface is assumed to have complete displacement compatibility unless a SLIDing card is input, in which case only normal displacement compatibility is assumed.

The ELEMents card and/or the POINTs card are included in SURFace input only to designate a subset of that surface.

Input on the ELEMents and POINTs cards may be continued on more than one card.

5. Boundary Condition Set Input

The boundary condition set section must be repeated for each new boundary condition.

<u>Keyword</u>	<u>Type of Input</u>	<u>Input</u>
** <u>BCSEt</u>		
<u>ID</u>	Alphanumeric	Boundary condition set name
<u>GMR</u>	Alphanumeric	Region name
<u>VALUe</u>		
<u>RELAtion</u>		
<u>SURFace</u>	Alphanumeric	Surface name
<u>ELEMents</u>	Numeric	Element number(s)
<u>POINTs</u>	Numeric	Node number(s)
<u>TIMES</u>	Numeric	Input time value(s)
<u>LOCAL</u>		
<u>GMR</u>	Alphanumeric	Region name
<u>SURFace</u>	Alphanumeric	Surface name
<u>ELEMents</u>	Numeric	Element number(s)
<u>POINTs</u>	Numeric	Node number(s)
<u>DISPLacement</u>	Numeric	Component value
<u>SPLIst</u>	Numeric	Source point value(s) <u>OR</u> ALL <u>OR</u> SAME
<u>T</u>	Numeric	Time point identifier, displacement value(s)
<u>RIGId</u>	Numeric	Component value
<u>SPRIng</u>	Numeric	Component value, spring value

TRACTION

SPLIST	Numeric	Source point value(s) <u>or</u> ALL <u>or</u> SAME
T	Numeric	Time point identifier, traction value(s)

The ELEMENTS card and/or the POINTS card are included in SURFACE input only to designate a subset of that surface.

The TIMES card must be omitted in a boundary condition set which contains a RIGID card. If the value(s) on the TIMES card differ from those values in the case control input, the output is calculated by linear interpolation. In the case of time independence (i.e., the TIMES card is omitted) the time point identifier on the T card must be 1 (one).

The LOCAL card designates input in the outward normal direction. The component value on the DISPLACEMENT, RIGID, SPRING, or TRACTION card must be 1 (one). Care must be taken not to mix global and local coordinate systems on a particular element. Care must also be taken not to input conflicting components on a particular node in a particular element.

The VALUE card should be included with the DISPLACEMENT card, the RIGID card, or the TRACTION card. The RELATION card should be included with the SPRING card.

Either RIGID input, or SPRING input, or TRACTION input must be included in a boundary condition set. This input set may be included up to three times (once for each component) in a boundary condition set. However, different boundary condition types may not be mixed in a boundary condition set.

The SPLIST card indicates the order in which the values are to be input on the T cards. The input may be in either of three forms:

- nodal values

- ALL to indicate that a single constant value is to be input
- SAME to use the previous source point list within the current boundary condition set (this option may not be used for the first source point list in the current boundary condition set).

Input on the ELEMents, POINTs, SPList, and TIMEs cards may be continued on more than one card. Input on the T card may be continued on more than one card, including the time point identifier on each card.

5.2 Sample Input

The following pages contain a sample data input for Composite-BEST for a cube with five inserts in tension. Note the simplicity of the input section for inserts. Each insert may contain a number of linear or quadratic elements. The keyword ELEMENTS is used before the definition of each distinct (non-connected) insert.

```

**CASE
  TITLE      CUBE WITH INSERT UNDER TENSION
  TIMES      1.
  RESTART    WRITE
**MATE
  ID MAT1
  TEMP 70.0
  EMOD 100.
  POIS 0.3
**GMR
  ID GHR1
  MAT MAT1
  TREF 70.0
  POINTS
    1      .0000      .0000      .0000
    2      .5000      .0000      .0000
    3      1.0000      .0000      .0000
    4      1.0000      .5000      .0000
    5      1.0000      1.0000      .0000
    6      .5000      1.0000      .0000
    7      .0000      1.0000      .0000
    8      .0000      .5000      .0000
  1001     .0000      .0000      .5000
  1002     .5000      .0000      .5000
  1003     1.0000      .0000      .5000
  1004     1.0000      .5000      .5000
  1005     1.0000      1.0000      .5000
  1006     .5000      1.0000      .5000
  1007     .0000      1.0000      .5000
  1008     .0000      .5000      .5000
  2001     .0000      .0000      1.0000
  2002     .5000      .0000      1.0000
  2003     1.0000      .0000      1.0000
  2004     1.0000      .5000      1.0000
  2005     1.0000      1.0000      1.0000
  2006     .5000      1.0000      1.0000
  2007     .0000      1.0000      1.0000
  2008     .0000      .5000      1.0000
SURFACE SURF11
  TYPE QUAD
  ELEMENTS
    101      1      2      3  1003  2003  2002  2001  1001  1002
    102      3      4      5  1005  2005  2004  2003  1003  1004
    103      5      6      7  1007  2007  2006  2005  1005  1006
    104      7      8      1  1001  2001  2008  2007  1007  1008
    1         1      2      3      4      5      6      7      8
    201      2001  2002  2003  2004  2005  2006  2007  2008
NORMAL 201 +

```

```

INSERT 1000.
POINTS
3001 0.5 0.5 0.
3002 0.5 0.5 0.125
3003 0.5 0.5 0.25
3004 0.5 0.5 0.5
3005 0.5 0.5 0.75
3006 0.5 0.5 0.875
3007 0.5 0.5 1.0

```

```

TYPE QUAD
ELEMENTS
301 .1 3001 3002 3003
302 .1 3003 3004 3005
303 .1 3005 3006 3007

```

```

INTERIOR
POINTS
9002 .5 .1 0.5
9004 .5 .2 0.5
9006 .5 .3 0.5
9007 .5 .35 0.5
9010 .5 .375 0.5

```

```

**BCSET
ID BC1
GMR GMR1
SURFACE SURF11
ELEMENTS 104
DISP 1
SPLIST ALL
T 1 0.0

```

```

**BCSET
ID BC2
GMR GMR1
SURFACE SURF11
ELEMENTS 104
POINTS 1001 1007
DISP 3
SPLIST 1001 1007
T 1 0.0.

```

```

**BCSET
ID BC3
GMR GMR1
SURFACE SURF11
ELEMENTS 104
POINTS 8 2008
DISP 2
SPLIST 8 2008
T 1 0.0.

```

```

**BCSET
ID BC4
GMR GMR1
SURFACE SURF11
ELEMENTS 102
TRAC 1
SPLIST ALL
T 1 100.0

```


5.3 Output Description

The output from Composite-BEST is relatively straightforward. It consists of ten sections, as follows:

1. Complete echo of the input data set.
2. Summary of case control and material property input.
3. Complete definition for each GMR, including all surface insert nodes, surface and insert elements.
4. Complete summary for each interface and boundary condition set, including the elements and nodes affected.
5. Boundary solution (on an element basis), including displacements and tractions at each node of each element.
6. The resultant load on each element and on the entire GMR is calculated and printed.
7. Solution for the displacements and tractions at the Insert/Matrix composite interface (on an element basis).
8. Displacement, stress and strain on a nodal basis, at all surface nodes, for each GMR.
9. Displacements at interior nodes.
10. Stresses at interior nodes.

A sample output is shown on the following pages for the data input that was given in Section 5.2.

5.4 Sample Output

ORIGINAL PAGE IS
OF POOR QUALITY

**** CASE CONTROL INPUT ****

JOB TITLE CUBE WITH INSERT UNDER TENSION
TIMES FOR SOLUTION: 1.0000000

BOUNDARY RESTART : 1

BOUNDARY INTEGRATION EPSILON: .00100000
INTERIOR INTEGRATION EPSILON: .00100000

**** MATERIAL INPUT ****

MATERIAL NAME: MAT1

ELASTIC

POISSONS RATIO: .3000

 TEMP ALPHA E
.70000E+02 .00000E+00 .10000E+03

**** GMR INPUT ****

REGION 1
NAME GMR1 MATERIAL MAT1

REFERENCE TEMPERATURE 70.00
INITIAL TEMPERATURE OF GMR .00

NODES	57	ELEMENTS	6	SURFACES	1
SOURCE POINTS	45	CELLS	0	NOLE ELEMENTS	0
NUMBER OF INSERTS	1			INSERT ELEMENTS	3

COORDINATE LIST

NODE	X	Y	Z
1	.0000	.0000	.0000
2	.5000	.0000	.0000
3	1.0000	.0000	.0000
4	1.0000	.5000	.0000
5	1.0000	1.0000	.0000
6	.5000	1.0000	.0000
7	.0000	1.0000	.0000
8	.0000	.5000	.0000
1001	.0000	.0000	.5000
1002	.5000	.0000	.5000
1003	1.0000	.0000	.5000
1004	1.0000	.5000	.5000
1005	1.0000	1.0000	.5000
1006	.5000	1.0000	.5000
1007	.0000	1.0000	.5000
1008	.0000	.5000	.5000
2001	.0000	.0000	1.0000
2002	.5000	.0000	1.0000
2003	1.0000	.0000	1.0000

ORIGINAL PAGE IS
OF POOR QUALITY

2004	1.0000	.5000	1.0000
2005	1.0000	1.0000	1.0000
2006	.5000	1.0000	1.0000
2007	.0000	1.0000	1.0000
2008	.0000	.5000	1.0000
3001	.5000	.5000	.0000
3002	.5000	.5000	.1250
3003	.5000	.5000	.2500
3004	.5000	.5000	.5000
3005	.5000	.5000	.7500
3006	.5000	.5000	.8750
3007	.5000	.5000	1.0000
9002	.5000	.1000	.5000
9004	.5000	.2000	.5000
9006	.5000	.3000	.5000
9007	.5000	.3500	.5000
9010	.5000	.3750	.5000

COORDINATE LIST OF NODES GENERATED BY GPBEST

NODE	X	Y	Z
73001	.5000	.6000	.0250
73002	.5000	.6000	.1250
73003	.5000	.6000	.2500
73004	.5000	.6000	.5000
73005	.5000	.6000	.7500
73006	.5000	.6000	.8750
73007	.5000	.6000	.9750
83001	.4134	.4500	.0250
83002	.4134	.4500	.1250
83003	.4134	.4500	.2500
83004	.4134	.4500	.5000
83005	.4134	.4500	.7500
83006	.4134	.4500	.8750
83007	.4134	.4500	.9750
93001	.5866	.4500	.0250
93002	.5866	.4500	.1250
93003	.5866	.4500	.2500
93004	.5866	.4500	.5000
93005	.5866	.4500	.7500
93006	.5866	.4500	.8750
93007	.5866	.4500	.9750

SURFACE SURF11 QUADRATIC VARIATION

ELEMENT	NODES								
101	1	2	3	1001	2003	2002	2001	1001	1002
102	3	4	5	1005	2005	2004	2003	1003	1004
103	5	6	7	1007	2007	2006	2005	1005	1006
104	7	8	1	1001	2001	2008	2007	1007	1008
1	1	8	7	6	5	4	3	2	
201	2001	2002	2003	2004	2005	2006	2007	2008	

INSERT ELEMENTS QUADRATIC VARIATION
ELASTIC MODULUS OF INSERTS .100000E+04

ELEMENT (INSERT 1)	RADIUS	NODES		
301	.1000	3001	3002	3003
302	.1000	3003	3004	3005
303	.1000	3005	3006	3007

SOURCE POINT LIST

1	2	3	4	5	6	7	8	1001	1002	1003	1004	1005	1006	1007	1008	2001	2002	2003	2004
2005	2006	2007	2008	73001	83001	93001	73002	83002	93002	73003	83003	93003	73004	83004	93004	73005	83005	93005	73006
83006	93006	73007	83007	93007															

ORIGINAL PAGE IS
OF POOR QUALITY

**** BOUNDARY CONDITION INPUT ****
GMR GMR1 SURFACE SURF11

ELEMENT LIST
104

SOURCE POINT LIST
7 8 1 1001 2001 2008 2007 1007 1008

COMPONENT 1 DISPLACEMENT INPUT

DATA VALUES:
.00000E+00 .00000E+00 .00000E+00 .00000E+00 .00000E+00 .00000E+00 .00000E+00
.00000E+00

**** BOUNDARY CONDITION INPUT ****
GMR GMR1 SURFACE SURF11

ELEMENT LIST
104

SOURCE POINT LIST
1001 1007

COMPONENT 3 DISPLACEMENT INPUT

DATA VALUES:
.00000E+00 .00000E+00

**** BOUNDARY CONDITION INPUT ****
GMR GMR1 SURFACE SURF11

ELEMENT LIST
104

SOURCE POINT LIST
8 2008

COMPONENT 2 DISPLACEMENT INPUT

DATA VALUES:
.00000E+00 .00000E+00

**** BOUNDARY CONDITION INPUT ****
GMR GMR1 SURFACE SURF11

ELEMENT LIST
102

SOURCE POINT LIST
3 4 5 1005 2005 2004 2003 1003 1004

COMPONENT 1 TRACTION INPUT

DATA VALUES:
10000E+03 10000E+03 10000E+03 10000E+03 10000E+03 10000E+03 10000E+03 10000E+03
10000E+03

MATRIX DECOMPOSITION - DIAGONAL BLOCK 1
CONDITION NUMBER 13387E+04

ORIGINAL PAGE IS
OF POOR QUALITY

JOB TITLE: CUBE WITH INSERT UNDER TENSION
BOUNDARY SOLUTION AT TIME = 1.0000 FOR REGION = GHR1

ELEMENT	NODE NO.	X-DISPL.	Y-DISPL.	Z-DISPL.	X-TRAC.	Y TRAC.	Z TRAC.
101	1	.00000E+00	.15593E+00	.13754E+00	.00000E+00	.00000E+00	.00000E+00
101	2	.48021E+00	.12997E+00	.13419E+00	.00000E+00	.00000E+00	.00000E+00
101	3	.98866E+00	.17094E+00	.14960E+00	.00000E+00	.00000E+00	.00000E+00
101	1003	.97531E+00	.17747E+00	.32046E-06	.00000E+00	.00000E+00	.00000E+00
101	2003	.98866E+00	.17094E+00	-.14960E+00	.00000E+00	.00000E+00	.00000E+00
101	2002	.48021E+00	.12997E+00	-.13419E+00	.00000E+00	.00000E+00	.00000E+00
101	2001	.00000E+00	.15593E+00	-.13754E+00	.00000E+00	.00000E+00	.00000E+00
101	1001	.00000E+00	.15477E+00	.00000E+00	.00000E+00	.00000E+00	.00000E+00
101	1002	.47753E+00	.13734E+00	.57255E-06	.00000E+00	.00000E+00	.00000E+00
102	3	.98866E+00	.17094E+00	.14960E+00	.10000E+03	.00000E+00	.00000E+00
102	4	.93793E+00	-.14762E-02	.13883E+00	.10000E+03	.00000E+00	.00000E+00
102	5	.98891E+00	-.17426E+00	.14839E+00	.10000E+03	.00000E+00	.00000E+00
102	1005	.97565E+00	-.17932E+00	.15470E-06	.10000E+03	.00000E+00	.00000E+00
102	2005	.98891E+00	-.17426E+00	-.14839E+00	.10000E+03	.00000E+00	.00000E+00
102	2004	.93793E+00	-.14761E-02	-.13883E+00	.10000E+03	.00000E+00	.00000E+00
102	2003	.98866E+00	.17094E+00	-.14960E+00	.10000E+03	.00000E+00	.00000E+00
102	1003	.97531E+00	.17747E+00	.32046E-06	.10000E+03	.00000E+00	.00000E+00
102	1004	.92675E+00	-.72162E-03	.45097E-06	.10000E+03	.00000E+00	.00000E+00
103	5	.98891E+00	-.17426E+00	.14839E+00	.00000E+00	.00000E+00	.00000E+00
103	6	.48072E+00	-.13313E+00	.13248E+00	.00000E+00	.00000E+00	.00000E+00
103	7	.00000E+00	-.15675E+00	.13696E+00	.00000E+00	.00000E+00	.00000E+00
103	1007	.00000E+00	-.15487E+00	.00000E+00	.00000E+00	.00000E+00	.00000E+00
103	2007	.00000E+00	-.15675E+00	-.13696E+00	.00000E+00	.00000E+00	.00000E+00
103	2006	.48072E+00	-.13313E+00	-.13247E+00	.00000E+00	.00000E+00	.00000E+00
103	2005	.98891E+00	-.17426E+00	-.14839E+00	.00000E+00	.00000E+00	.00000E+00
103	1005	.97565E+00	-.17932E+00	.15470E-06	.00000E+00	.00000E+00	.00000E+00
103	1006	.47808E+00	-.13787E+00	.47441E-06	.00000E+00	.00000E+00	.00000E+00
104	7	.00000E+00	-.15675E+00	.13696E+00	-.89836E+02	.00000E+00	.00000E+00
104	8	.00000E+00	.00000E+00	.14814E+00	-.10162E+03	.18828E+00	.00000E+00
104	1	.00000E+00	.15593E+00	.13754E+00	-.89513E+02	.00000E+00	.00000E+00
104	1001	.00000E+00	.15477E+00	.00000E+00	-.89810E+02	.00000E+00	-.10514E-03
104	2001	.00000E+00	.15593E+00	-.13754E+00	-.89513E+02	.00000E+00	.00000E+00
104	2008	.00000E+00	.00000E+00	-.14814E+00	-.10162E+03	.18828E+00	.00000E+00
104	2007	.00000E+00	-.15675E+00	-.13696E+00	-.89836E+02	.00000E+00	.00000E+00
104	1007	.00000E+00	-.15487E+00	.00000E+00	-.90021E+02	.00000E+00	-.94079E-04
104	1008	.00000E+00	.89522E-04	.50108E-06	-.10605E+03	.00000E+00	.00000E+00

JOB TITLE: CUBE WITH INSERT UNDER TENSION
BOUNDARY SOLUTION AT TIME = 1.0000 FOR REGION = GHR1

ELEMENT	NODE NO.	X-DISPL.	Y-DISPL.	Z-DISPL.	X-TRAC.	Y TRAC.	Z TRAC.
1	1	.00000E+00	.15593E+00	.13754E+00	.00000E+00	.00000E+00	.00000E+00
1	8	.00000E+00	.00000E+00	.14814E+00	.00000E+00	.00000E+00	.00000E+00
1	7	.00000E+00	-.15675E+00	.13696E+00	.00000E+00	.00000E+00	.00000E+00
1	6	.48072E+00	-.13313E+00	.13248E+00	.00000E+00	.00000E+00	.00000E+00
1	5	.98891E+00	-.17426E+00	.14839E+00	.00000E+00	.00000E+00	.00000E+00
1	4	.93793E+00	-.14762E-02	.13883E+00	.00000E+00	.00000E+00	.00000E+00
1	3	.98866E+00	.17094E+00	.14960E+00	.00000E+00	.00000E+00	.00000E+00
1	2	.48021E+00	.12997E+00	.13419E+00	.00000E+00	.00000E+00	.00000E+00
201	2001	.00000E+00	.15593E+00	-.13754E+00	.00000E+00	.00000E+00	.00000E+00
201	2002	.48021E+00	.12997E+00	-.13419E+00	.00000E+00	.00000E+00	.00000E+00
201	2003	.98866E+00	.17094E+00	-.14960E+00	.00000E+00	.00000E+00	.00000E+00
201	2004	.93793E+00	-.14761E-02	-.13883E+00	.00000E+00	.00000E+00	.00000E+00
201	2005	.98891E+00	-.17426E+00	-.14839E+00	.00000E+00	.00000E+00	.00000E+00
201	2006	.48072E+00	-.13313E+00	-.13247E+00	.00000E+00	.00000E+00	.00000E+00
201	2007	.00000E+00	-.15675E+00	-.13696E+00	.00000E+00	.00000E+00	.00000E+00
201	2008	.00000E+00	.00000E+00	-.14814E+00	.00000E+00	.00000E+00	.00000E+00

ORIGINAL PAGE IS
OF POOR QUALITY

JOB TITLE: CUBE WITH INSERT UNDER TENSION
LOAD CALCULATION AT TIME = 1.000000

LOADS FOR REGION GMR1

ELEMENT	X	Y	Z
101	.00000E+00	.00000E+00	.00000E+00
102	.10000E+03	.00000E+00	.00000E+00
103	.00000E+00	.00000E+00	.00000E+00
104	-.99659E+02	.41842E-01	-.22136E-04
1	.00000E+00	.00000E+00	.00000E+00
201	.00000E+00	.00000E+00	.00000E+00
LOAD BALANCE	.34092E+00	.41842E-01	-.22136E-04

JOB TITLE: CUBE WITH INSERT UNDER TENSION
INSERT ELEMENT SOLUTION AT TIME = 1.0000 FOR REGION = GMR1

ELEMENT	NODE NO.	X-TRAC.	Y TRAC.	Z TRAC.
301	73001	.89532E+00	.10010E+01	-.45449E+02
301	83001	.12852E+03	-.69704E+01	-.49540E+02
301	93001	.12607E+03	-.73593E+01	-.50428E+02
301	73002	.72226E+00	.96271E+01	-.10879E+02
301	83002	.11868E+03	-.28546E+01	-.77024E+01
301	93002	.11989E+03	-.29981E+01	-.83725E+01
301	73003	.29744E+00	.48065E+01	-.74677E+01
301	83003	.11874E+03	-.17167E+01	-.88572E+01
301	93003	.11874E+03	-.20814E+01	-.82263E+01
302	73003	.29744E+00	.48065E+01	-.74677E+01
302	83003	.11874E+03	-.17167E+01	-.88572E+01
302	93003	.11874E+03	-.20814E+01	-.82263E+01
302	73004	.14592E+00	.64886E+01	.27555E-03
302	83004	.11796E+03	-.24306E+01	.22600E-03
302	93004	.11746E+03	-.28693E+01	.36406E-03
302	73005	.29706E+00	.48068E+01	.74674E+01
302	83005	.11874E+03	-.17166E+01	.88575E+01
302	93005	.11874E+03	-.20819E+01	.82249E+01
303	73005	.29706E+00	.48068E+01	.74674E+01
303	83005	.11874E+03	-.17166E+01	.88575E+01
303	93005	.11874E+03	-.20819E+01	.82249E+01
303	73006	.72447E+00	.96234E+01	.10985E+02
303	83006	.11868E+03	-.28534E+01	.77065E+01
303	93006	.11989E+03	-.29956E+01	.83816E+01
303	73007	.89906E+00	.10029E+01	.45437E+02
303	83007	.12852E+03	-.69699E+01	.49527E+02
303	93007	.12607E+03	-.73594E+01	.50416E+02

JOB TITLE: CUBE WITH INSERT UNDER TENSION
INTERIOR DISPLACEMENT AT TIME = 1.0000 FOR REGION = GMR1

NODE	X DISPLACEMENT	Y DISPLACEMENT	Z DISPLACEMENT
9002	.475566E+00	.105777E+00	.636808E-06
9004	.473093E+00	.727447E-01	.765990E-06
9006	.470797E+00	.362568E-01	.979925E-06
9007	.469954E+00	.161879E-01	.114285E-05
9010	.469622E+00	.676120E-02	.125234E-05

JOB TITLE: CUBE WITH INSERT UNDER TENSION
INTERIOR STRESS AT TIME = 1.0000 FOR REGION = GMR1

NODE	SIGMA-XX	SIGMA-YY	SIGMA-ZZ	TAU-XY	TAU-YZ	TAU-XZ
9002	.997037E+02	.419311E+00	-.222586E+01	-.874776E+01	-.627650E+01	-.675488E+01
9004	.101083E+03	.131699E+00	-.343431E+01	-.832353E+01	-.512052E+01	-.624766E+01
9006	.106541E+03	.294053E-02	-.422035E+01	-.725881E+01	-.375639E+01	-.520628E+01
9007	.112658E+03	-.840790E-01	-.451955E+01	-.636016E+01	-.329232E+01	-.424838E+01
9010	.116245E+03	-.351612E+00	-.448963E+01	-.550159E+01	-.323272E+01	-.356346E+01

6. EXAMPLES OF COMPOSITE INSERT ANALYSIS

6.1 Introduction

In this section a number of examples are presented to verify and demonstrate the applications of the ceramic composite formulation for elastic fully-bonded inserts.

In the mesh diagrams of the models containing the inserts, a double line is used to indicate the centerline of the insert elements. The length of these segments are shown in proper proportion for the three-dimensional views, however, the radii of the inserts are not indicated on these diagrams. The double line is a symbolic representation of the insert elements and does not in any way indicate the diameter of the insert. Refer to the example description for the values of the radii.

Throughout this section consistent units are used in the definition of the examples. This means all lengths are defined in the same units and the tractions and the elastic moduli are defined in terms of these lengths as Force/length². No confusion should arise since the results are reported as non-dimensional quantities.

6.2 Cube With a Single Insert

The first test of the formulation is on a unit cube with a single insert through its center of radius 0.1. The cube is subjected to tension and shear in the direction parallel and perpendicular to the insert. The cube has a modulus of 100.0 and a Poisson ratio of 0.3. Consistent units are used for all information described in this problem. An insert with two different moduli of 1,000 and 10,000 is studied. The Poisson ratio of the insert is assumed to be the same as that of the cube.

The problem is analyzed by both the present formulation and by a full three-dimensional multi-region BEM approach. As shown in Fig. 6.2.1, the model for the insert formulation consists of fourteen quadratic boundary

elements and the insert contains three quadratic insert elements. The two-region, three-dimensional model shown in Fig. 6.2.2 contain twenty quadratic boundary elements in the first region and sixteen in the second. Note 9-noded elements are used in describing the insert and hole to accurately capture the curvilinear geometry.

In Fig. 6.2.3, the profile of the end displacement of the cube under a uniform normal traction of 100.0 (in parallel with the insert) is shown. The present formulation is in good agreement with the full three-dimensional results for $E_i/E = 10$. For the case $E_i/E = 100$, the insert formulation exhibits greater stiffness than the 3-D results. This difference is contributed by the way the load is distributed from the insert to the composite matrix. In the full 3-D model, the applied traction and the resulting reactions at the fixed end act directly on the end of the insert. In the composite formulation, the insert is assumed not to intersect the boundary surface and therefore the insert is moved back slightly from the end of the cube. The load is therefore transferred through the composite matrix to the end of the insert and to its sides in a manner that is slightly different from the full 3-D analysis.

In Fig. 6.2.4, the stress distribution through the center of the cube (from A to B as indicated in the figure) is shown. Again the results are very good for $E_i/E = 10$, and deviates slightly from the full 3-D results in the second case.

In Figs 6.2.5 and 6.2.6, the lateral displacements along the side of the cube are shown for a cube subjected to a shear traction of 100. For the case of applied shear perpendicular to the insert (Fig. 6.2.5), the results for both the insert and full 3-D model show good agreement. Once again a slight deviation is observed for $E_i/E = 100$. In the case of the shear traction in the plane of the insert (Fig. 6.2.6) the insert has

little effect on the displacement (as anticipated) and all results fall in close proximity.

6.3 Lateral Behavior of a Cube With Multiple Inserts

Existing methods of analysis of composite material based on mechanics of materials have been relatively successful in predicting the behavior of composite material for loading in the longitudinal direction. The properties perpendicular to the direction of the fibers are not so readily predictable by present means. The focus of the present example concerns this lateral behavior.

Four cubes (Fig. 6.3.1) with one, two, five and nine inserts are fixed with a roller boundary condition on one side and subjected to a uniform traction, perpendicular to the inserts. The material properties, given in consistent units, are

$$\begin{array}{ll} E^{\text{insert}} = 10000. & E^{\text{matrix}} = 100. \\ \nu^{\text{insert}} = 0.3 & \nu^{\text{matrix}} = 0.3 \end{array}$$

For the cube with one and two inserts, the boundary mesh consists of two quadratic surface elements on each lateral side and four elements on the top and bottom. For the cubes with five and nine inserts, one additional element was added to the side with the applied traction and to the side with the roller boundary condition. The top and bottom faces contain six elements to match the pattern of the sides. In all cases, each insert contained three one-dimensional quadratic elements.

The profile for the end displacement for a cube with one insert and five inserts are shown in Figs. 6.3.2 and 6.3.3. The results seem to be in good agreement with the two-dimensional results. The 2-D results are approximations since plane stress is assumed. The 3-D solutions for the

one insert are within 2% error of the 2-D solution and within 3% for the case of 5 inserts.

Also shown in Fig. 6.3.4 are the average end displacements for the one, two, five and nine inserts. Results show good agreement with 2-D results. For one, two and five inserts, the solutions are within 2% error of the 2-D results and 6% for the case of nine inserts where the insert of volume to total volume ratio is 28.2%. The result is also displayed in a plot of Effective Modulus vs. Insert Volume Ratio in Fig. 6.2.5. The effective modulus is defined as the average stress/average strain. The three-dimensional results follow closely to the two-dimensional solution.

6.4 Thick Cylinder With Circumferential Insert Supports

The strength of a cylinder under internal pressure can be increased by adding stiff circumferential insert supports. In the present example, a three-dimensional, open ended thick cylinder with four inserts is analyzed. The inner and outer radii of the cylinder are 10 and 20 respectively, the thickness is 2 and the radius of the fully-bonded inserts is 0.5. By using roller boundary conditions on the faces of symmetry, only a fifteen degree slice of the thick cylinder needs to be modeled. As shown in Fig. 6.4.1, sixteen eight-noded quadratic boundary elements are used to define the sides of the model, a nine-noded element is used on both the internal and external faces of the cylinder, and three insert elements are used per insert. Note, the inserts in this problem are curvilinear in geometry. The elastic modulus of the cylinder is assumed to be 100, and the effect of inserts with five different moduli of 100, 250, 500, 750 and 1000 is studied. The Poisson ratio is 0.3 for both the composite matrix and insert, and the internal pressure in the cylinder is 100.

Results from a multi-region, axisymmetric BEM analysis were used for comparison with the 3-D insert results of the present example. The

axisymmetric model consists of twenty quadratic boundary elements on the outer surface, and six boundary elements per hole and per insert (Fig. 6.4.2). The radial displacement through the thick cylinder along the top face is shown in Fig. 6.4.3 for all five moduli. The displacement for the composites with low E_i/E ratios are in good agreement with the axisymmetric results, and diverge slightly for higher E_i/E ratios. In Fig. 6.4.4, the circumferential stress is shown for the same points along the top edge. This stress is smooth for the homogeneous case ($E_i/E = 1.0$) and exhibits increasing fluctuations as the E_i/E ratio increases and the inserts take on more of the load. The circumferential stress of the 3-D insert model is in good agreement with the axisymmetric results for all cases. In Fig. 6.4.5, the radial stress is displayed for the two models. The inserts have little effect on this stress and the curves for the five moduli fall close together for both approaches.

6.5 Cube With Multiple Inserts With Random Orientation

In an attempt to analyze a material with a random fiber structure, cubes with multiple inserts oriented in random directions are studied. The cubes are of unit length and have four boundary elements per side (Fig. 6.5.1a). Randomly oriented fibers of variable length with radii of 0.05 are placed in five cubes in quantities of 5, 10, 15, 20, and 25 (Fig. 6.5.1b-f). Three cases of material properties are considered for each cube. The modulus of the composite matrix is 100 for all cases, however, the modulus of the inserts are 500, 10,000 and 200,000 in the three cases studied. Poisson's ratio is uniformly 0.3 throughout. Roller boundary conditions are employed on three adjacent sides and a uniform normal traction of 100 is applied to a fourth face.

The normal end displacement at the center of the face on the side with

the applied traction is plotted against the number of inserts in a cube for the three materials (Fig. 6.5.2). The displacement decreases with increasing number of inserts per cube and increasing E_i/E values as expected.

6.6 A Beam With Insert Reinforcement in Bending

In the last example, the applicability of the present formulation to the study of the micromechanical behavior of the ceramic composite is apparent. The present formulation, however, is equally applicable to typical problems encountered by civil engineers. Using Composite-BEST reinforced concrete can now be modeled exactly as a three-dimensional body and studied in detail for the first time. The present example considers a reinforced concrete beam. Here the concrete plays the role of the composite matrix and the reinforcement bars play the role of the fiber insert. In Fig. 6.6.1, a 4x1x1 beam with four inserts is modeled using twenty-eight quadratic boundary elements. The ratio of insert modulus to matrix modulus (E_i/E) is studied for a range of values between 1 and 100. The Poisson ratio is 0.3 for both the beam and reinforced rods.

The beam is completely fixed at one end and a downward shear traction of 100 is applied to the other end. The non-dimensional vertical displacement of the end obtained from the analysis is shown in Fig. 6.6.2 as a function of E_i/E . The non-dimensional displacement is defined here as the end displacement of the reinforced beam divided by the displacement of a homogeneous beam under similar conditions.

The end displacement obtained from the mechanics of material solution is also displayed in Fig. 6.6.2 in non-dimensional form. The curvature of the two plots are very similar but differ in magnitude. This difference is contributed to the fact that although the mechanics of material solution accounts for the stiffening due to the inserts, it does not include the

effect of interaction between inserts.

6.7 Laminated Fiber Composite

A laminated composite fabricated from a fiber composite material is shown in Fig. 6.7.1. The fiber composite is constructed with a single row of fully-bonded fibers oriented in the same direction. A two-ply laminate is then constructed from the fiber composite with the fibers of the two layers oriented at 90° angles. A boundary element model created for the study of this material is shown in Fig. 6.7.2. A small slice containing two inserts in each layer is used. The model consists of two regions. The outer surface of each region is modeled with sixteen quadratic boundary elements and each insert contains two quadratic insert elements. The interface between the two regions is assumed to be a perfect bond, however, the present version of the program allows for sliding and spring connections also.

The composite structure is subjected to bi-axial tension. This is accomplished with normal tractions of 100 applied to two adjacent roller boundary conditions applied to the opposite ends. The elastic modulus of the composite matrix of both regions are assumed to be 100, and the moduli of the inserts vary between 100 and 10,000. The Poisson ratio is 0.3 for both the composite matrix and inserts at all times.

Figure 6.7.3 displays the displacement as a function of insert moduli for a point on the interface at the corner of the plate adjacent to the sides with the applied traction. The material exhibits less displacement as the modulus is increased, as expected.

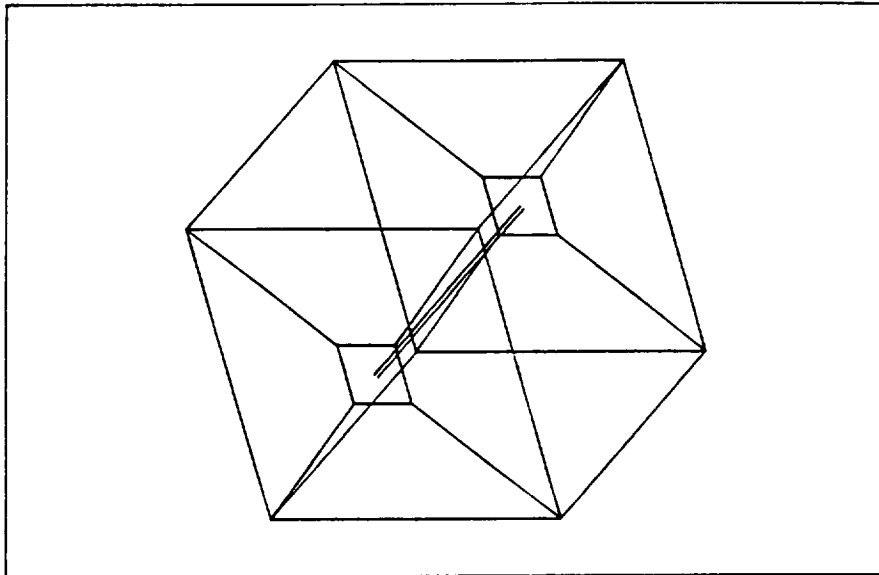


Fig. 6.2.1 Discretization of an Insert in a Unit Cube Utilizing Quadratic Insert Elements

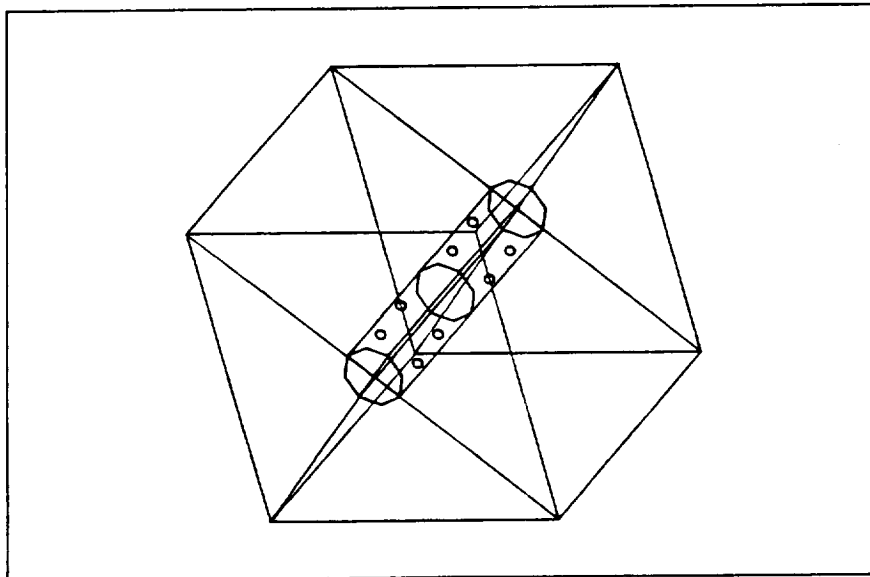


Fig. 6.2.2 Full Three-dimensional, Multi-region Discretization of an Insert in a Unit Cube

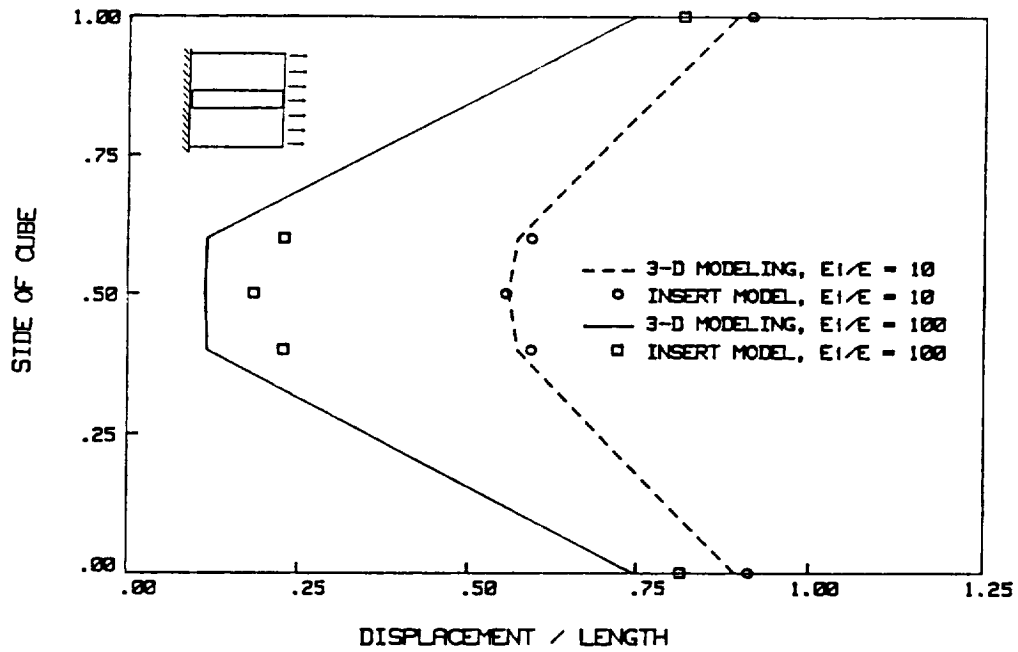


Fig. 6.2.3 Comparison of Displacement Profiles Between the Full 3-D Model and the Insert Element Model for the End of a Cube in Tension

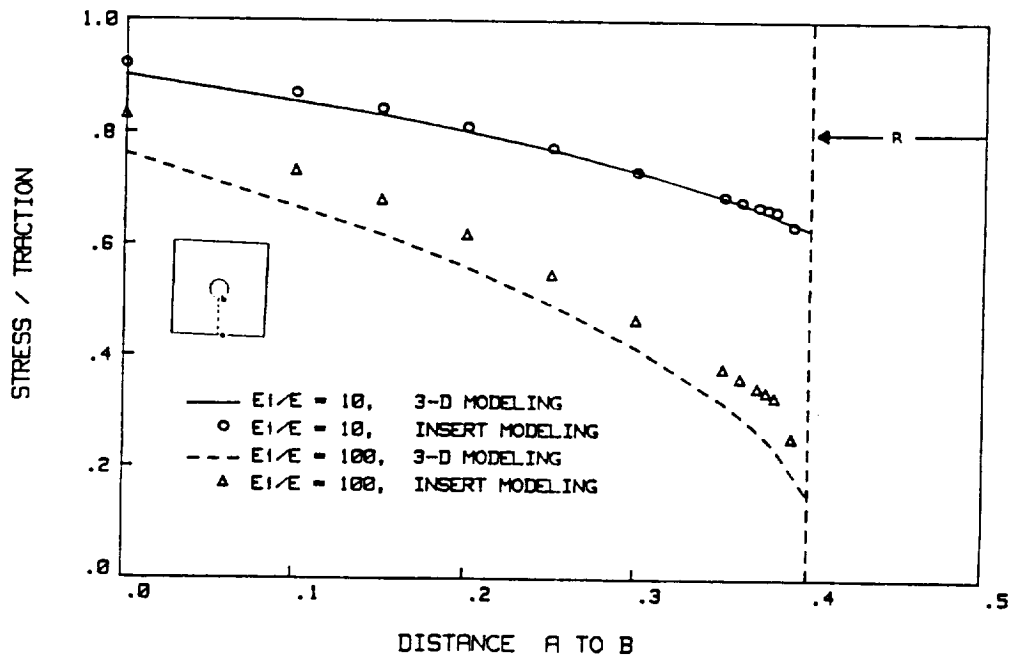


Fig. 6.2.4 Axial Stress Through the Cross Section of a Unit Cube in Tension with a Single Insert in Parallel with the Loading

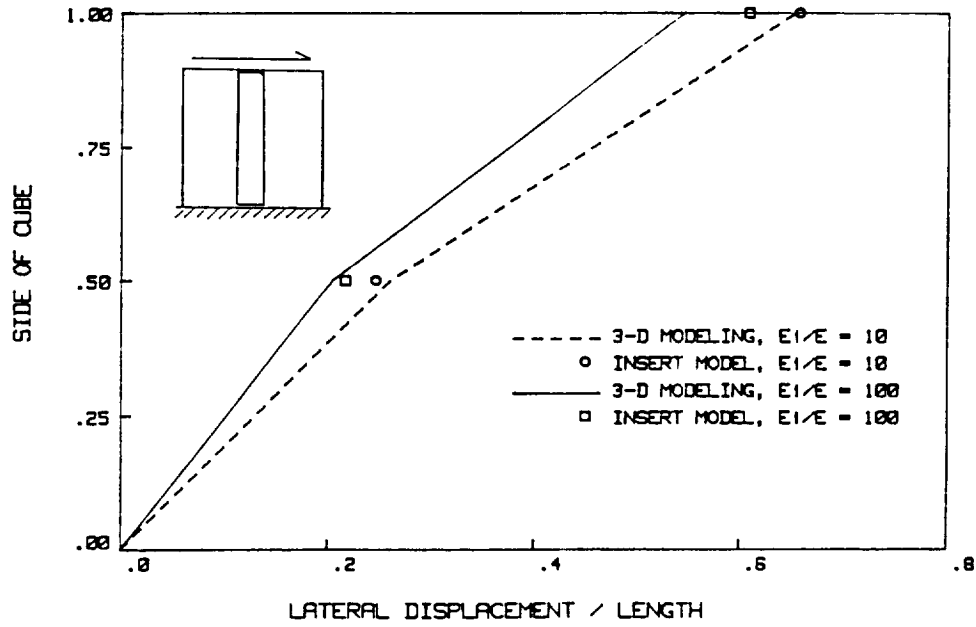


Fig. 6.2.5 Lateral Displacement Along a Side of a Cube Subjected to a Shear Force Perpendicular to an Insert

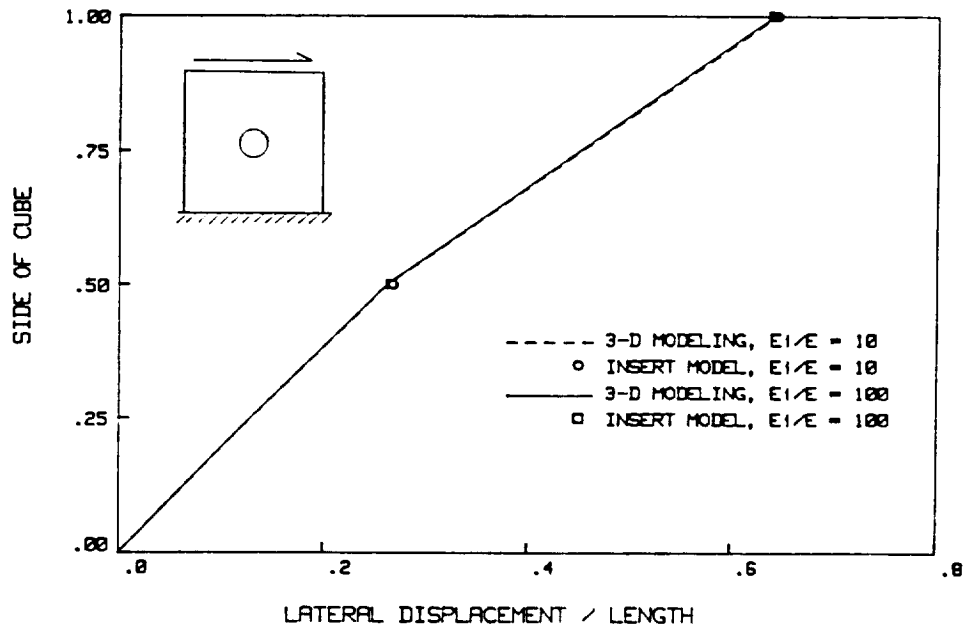


Fig. 6.2.6 Lateral Displacement Along a Side of a Cube Subjected to a Shear Force in the Cross-Plane of an Insert

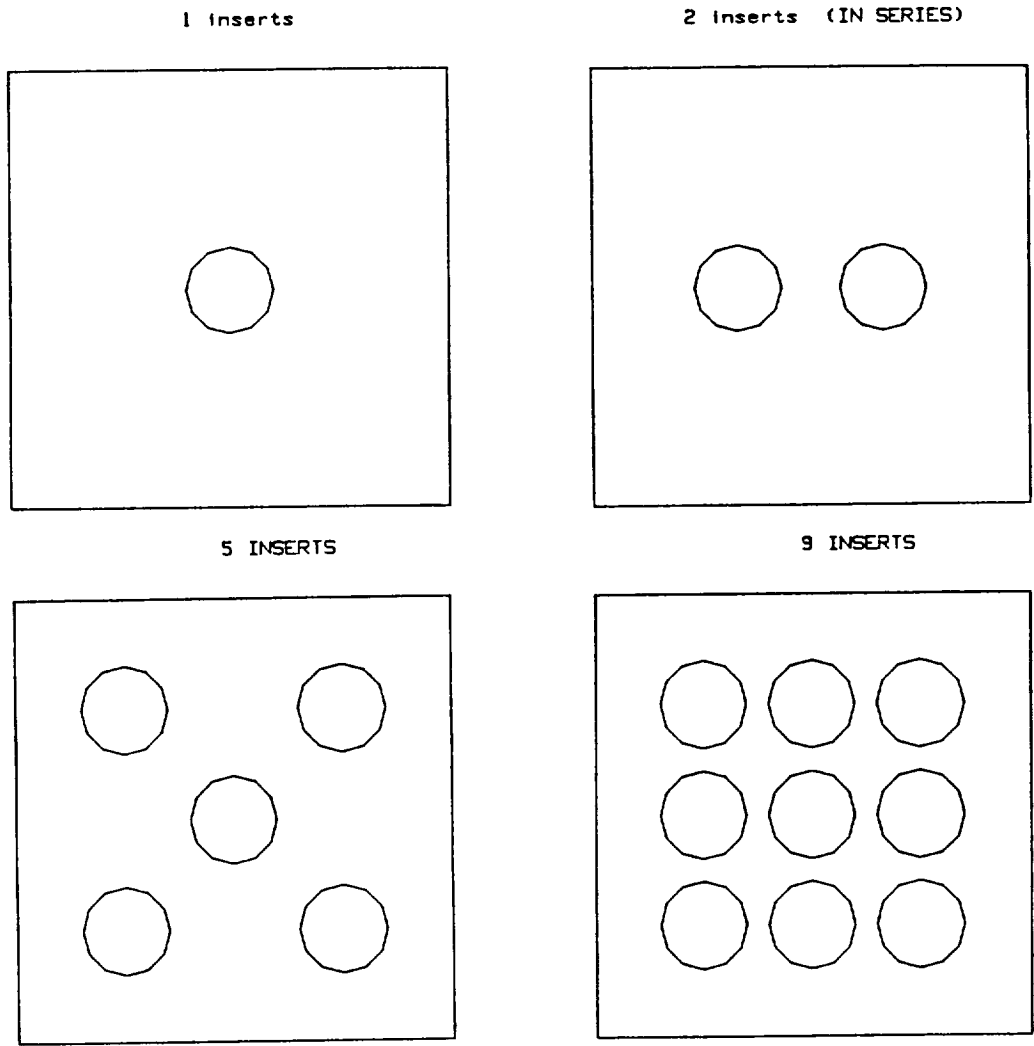


Fig. 6.3.1 Arrangement of Multiple Inserts in a Unit Cube Subjected to Lateral Tension

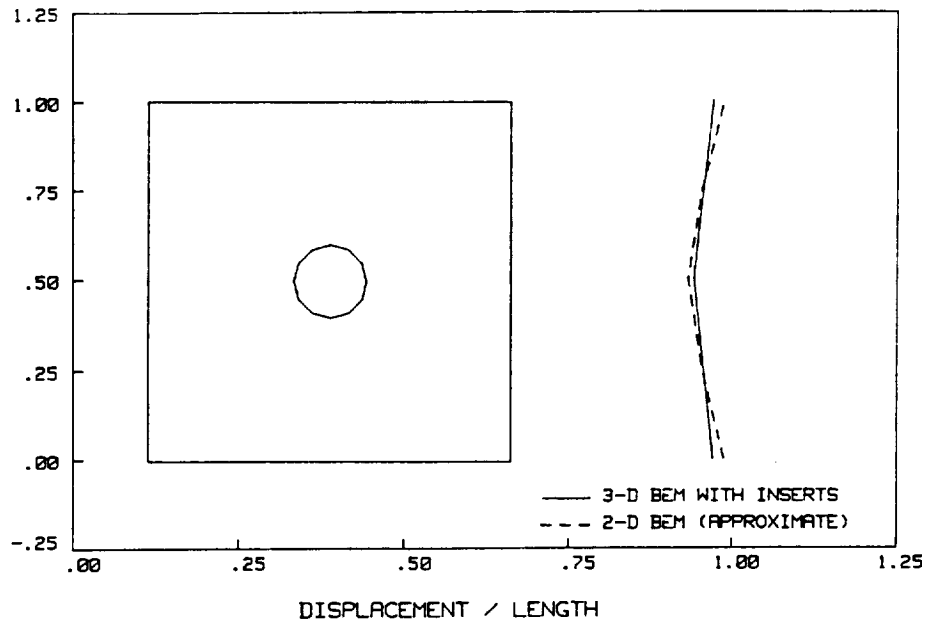


Fig. 6.3.2 Displacement Profile of a Cube with a Single Insert Under Lateral Tension

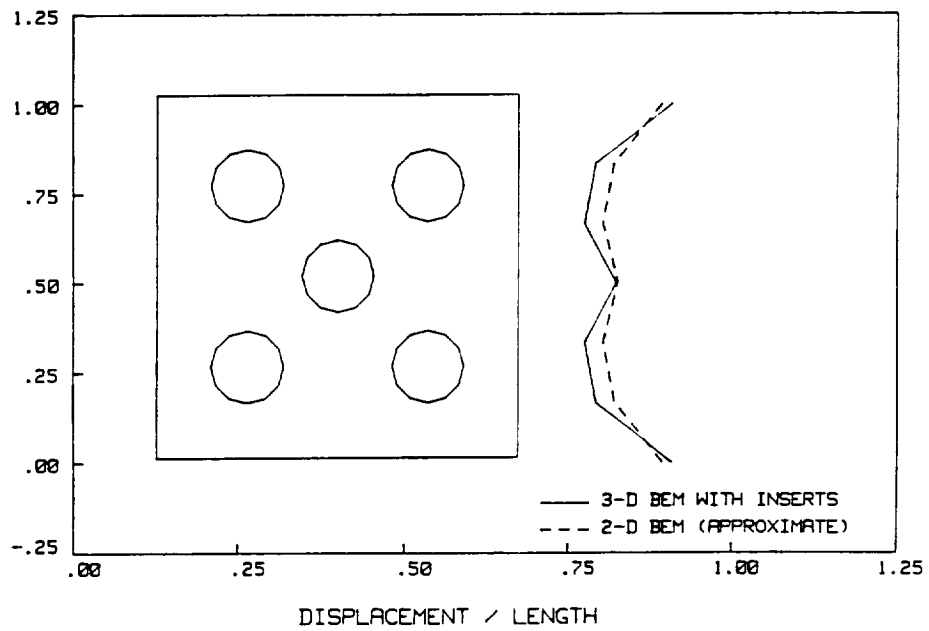


Fig. 6.3.3 Displacement Profile of a Cube with Five Inserts Under Lateral Tension

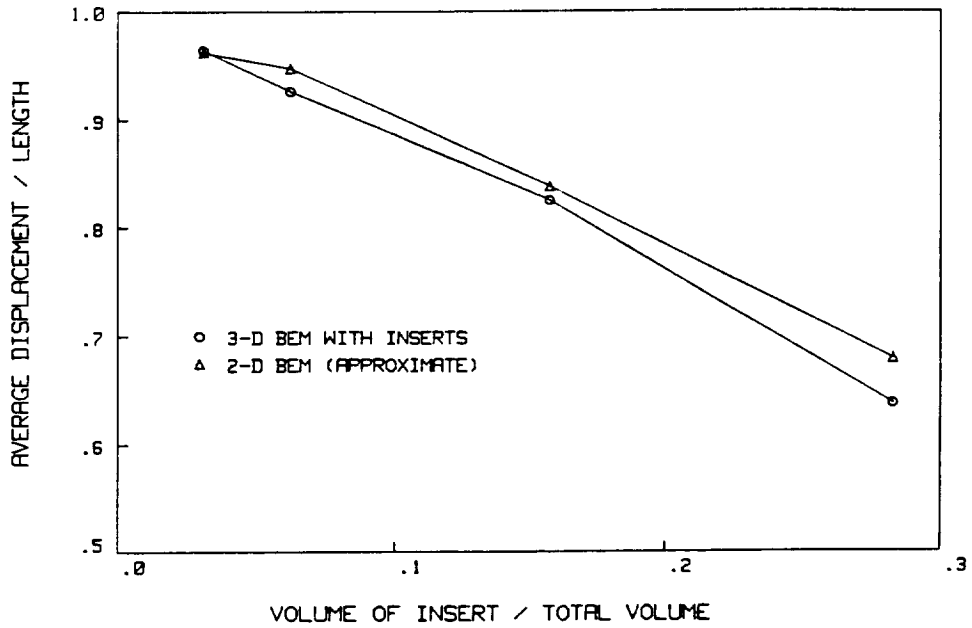


Fig. 6.3.4 Average End Displacement of a Cube Under Tension vs. the Volume of Insert to Total Volume Ratio

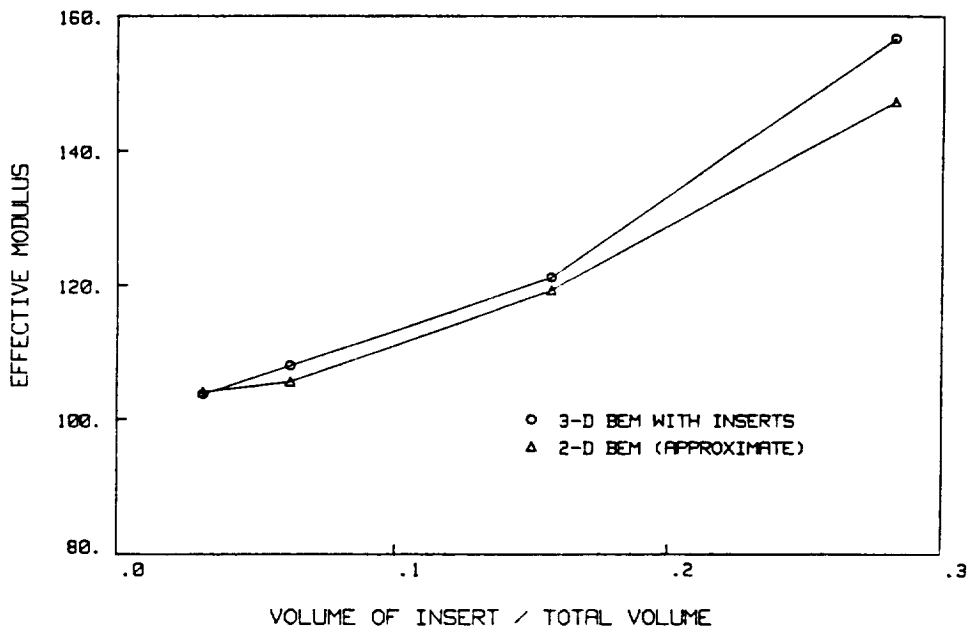


Fig. 6.3.5 Effective Transverse Modulus of a Cube as a Function of Insert Volume to Total Volume

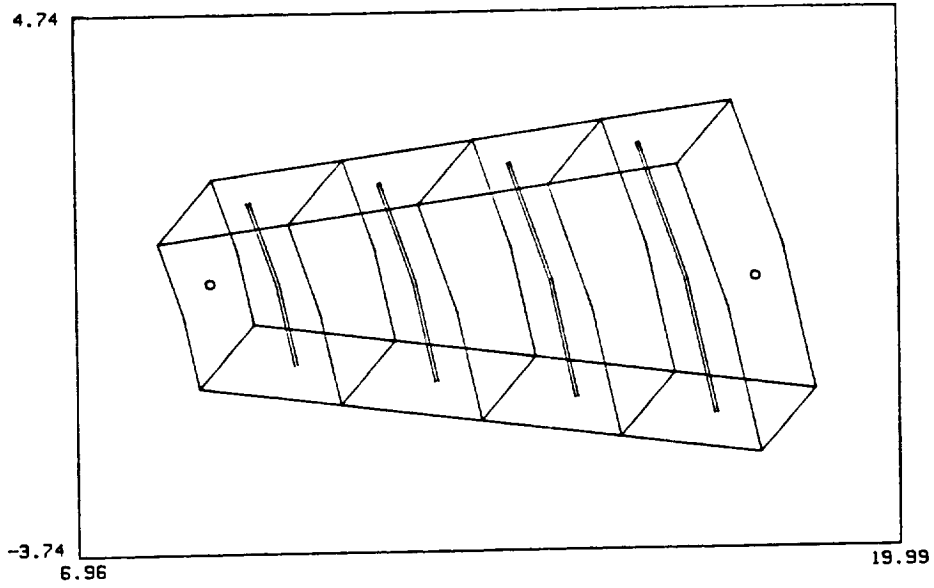


Fig. 6.4.1 Discretization of a Thick Cylinder with Four Inserts Utilizing Insert Elements

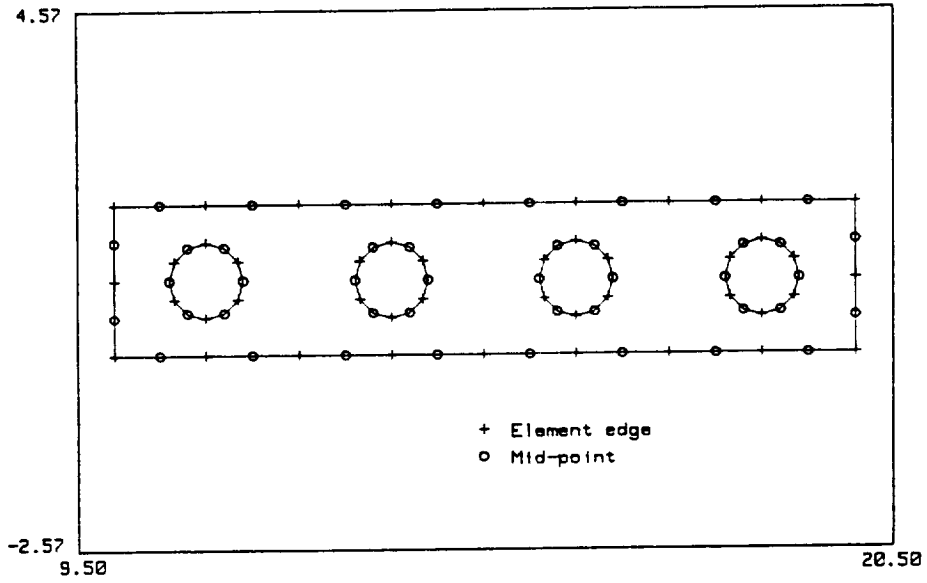


Fig. 6.4.2 Axisymmetric Multi-region, Discretization of a Thick Cylinder with Four Inserts

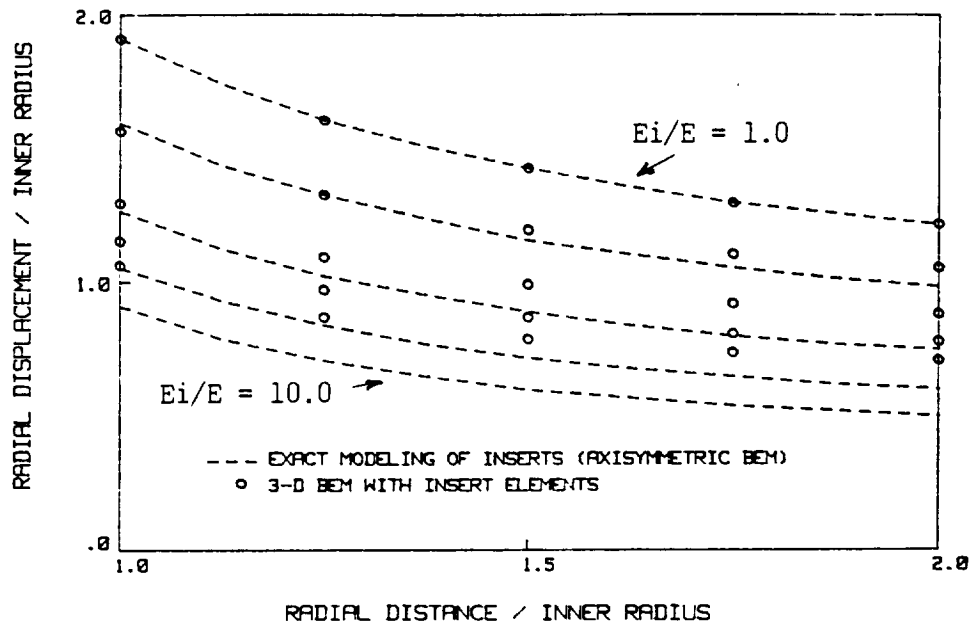


Fig. 6.4.3 Radial Displacement Through a Pressurized Thick Cylinder with Circumferential Inserts for $E_i/E = 1.0, 2.5, 5.0, 7.5, 10.0$

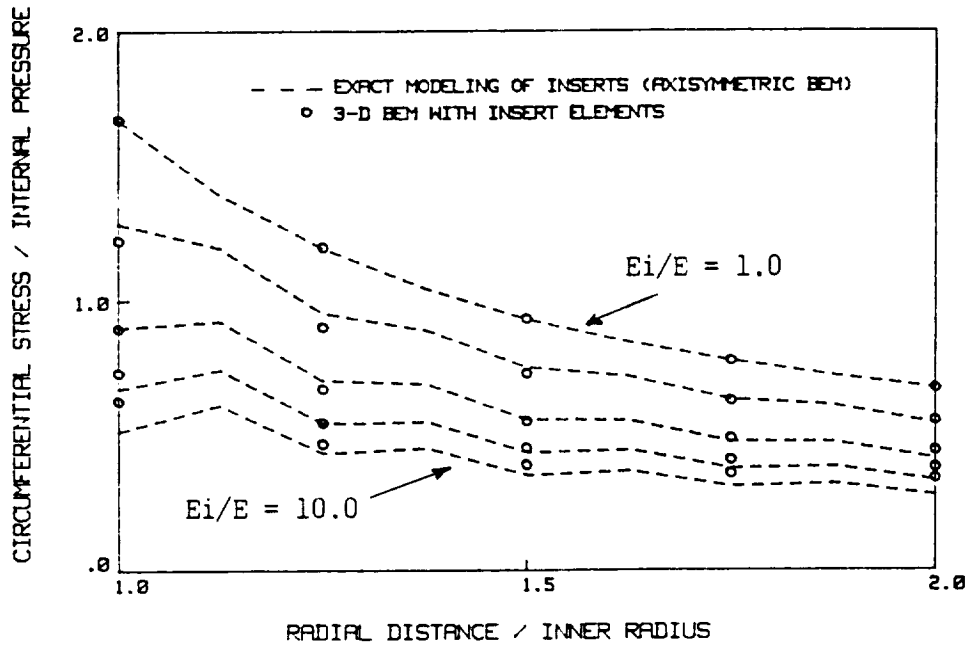


Fig. 6.4.4 Circumferential Stress Through a Pressurized Thick Cylinder with Circumferential Inserts for $E_i/E = 1.0, 2.5, 5.0, 7.5, 10.0$

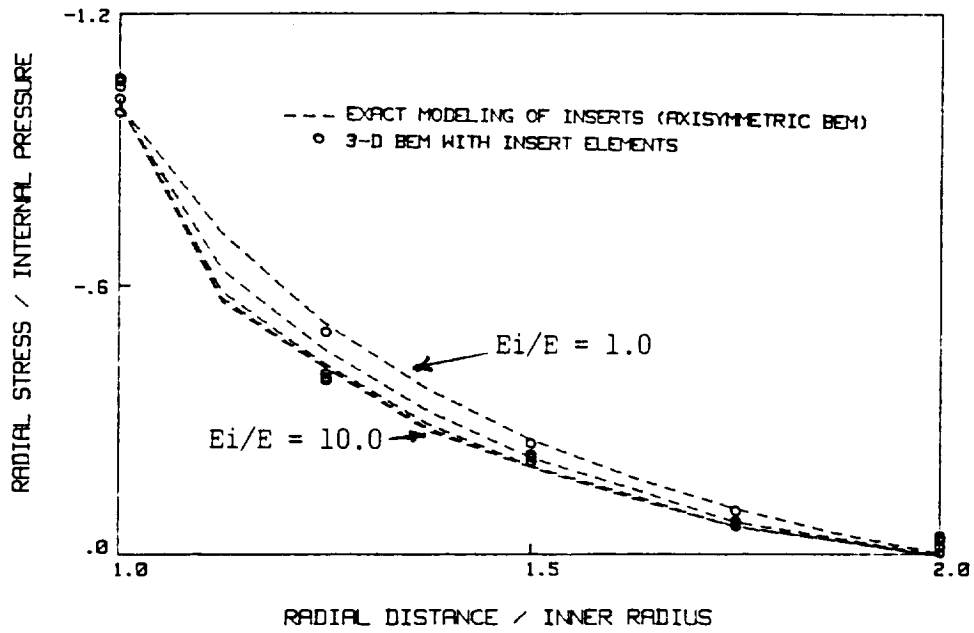


Fig. 6.4.5 Radial Stress Through a Pressurized Thick Cylinder with Circumferential Inserts for $E_i/E = 1.0, 2.5, 5.0, 7.5, 10.0$

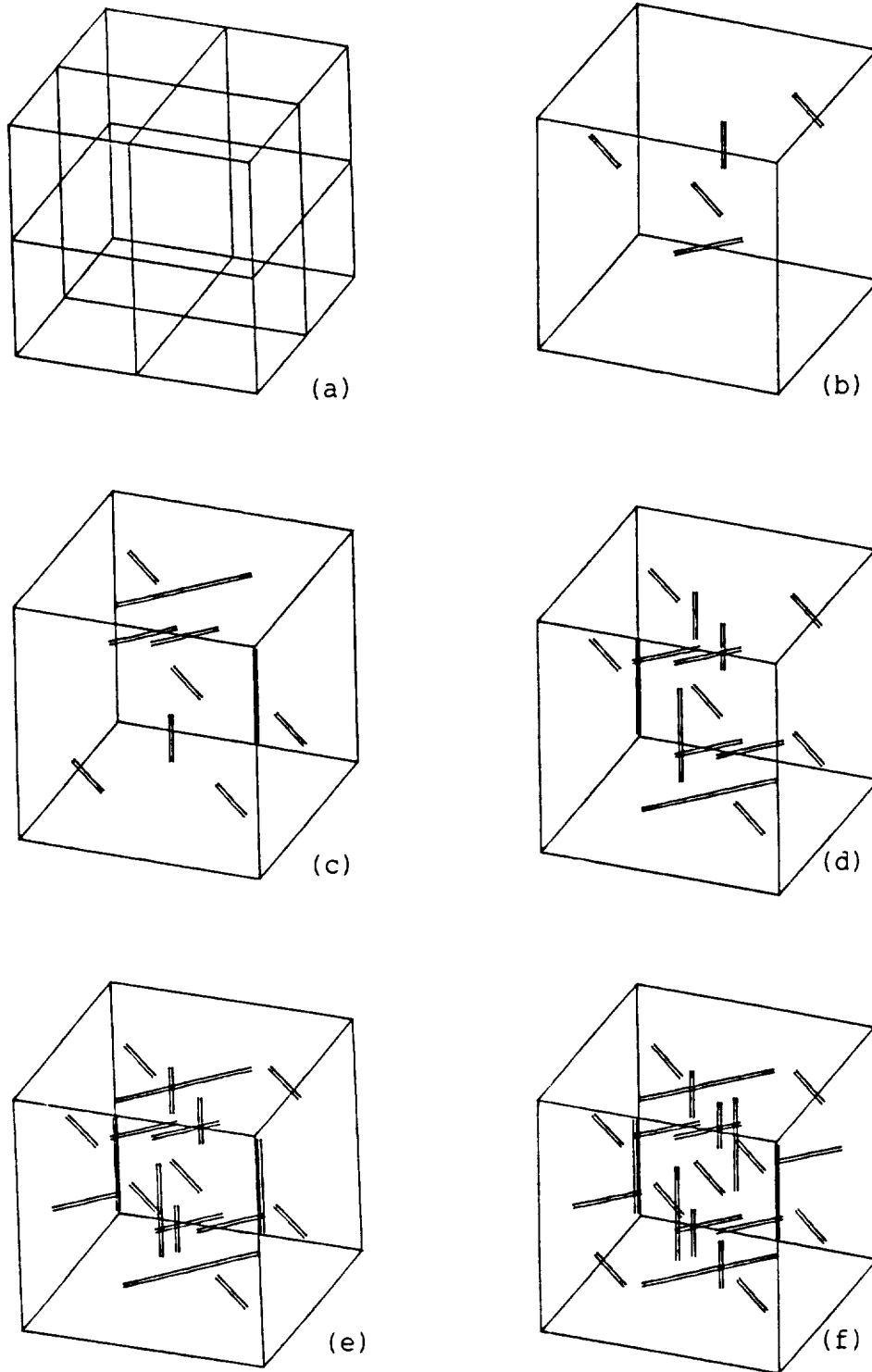


Fig. 6.5.1 (a) Surface Discretization of a Unit Cube Used in the Study of Random Oriented Inserts, (b-f) Orientation of Variable Length Inserts Within Unit Cubes Containing 5, 10, 15, 20, and 25 Inserts, respectively

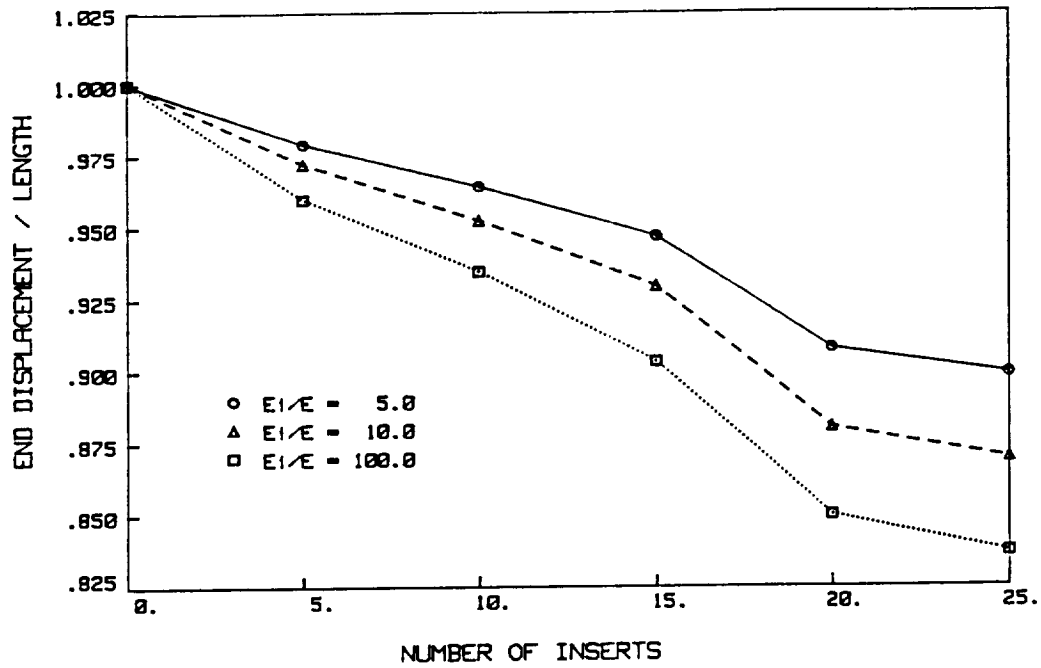


Fig. 6.5.2 End Displacement of a Unit Cube With Random Oriented Inserts of $E_i/E = 5.0, 10.0$ and 100.0

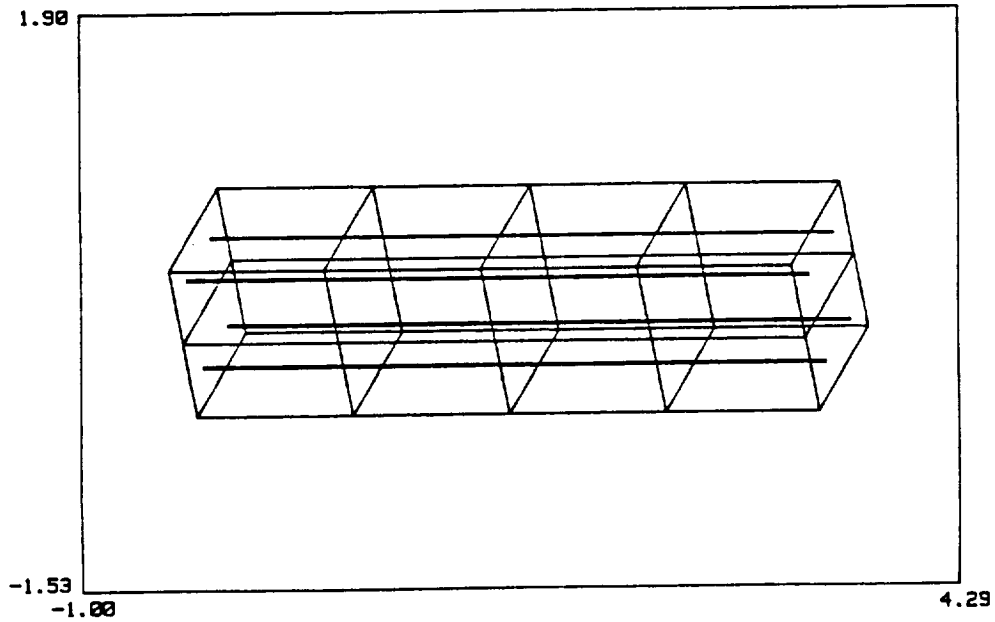


Fig. 6.6.1 Discretization of a Reinforced Beam Utilizing Quadratic Insert Elements to Model the Four Inserts

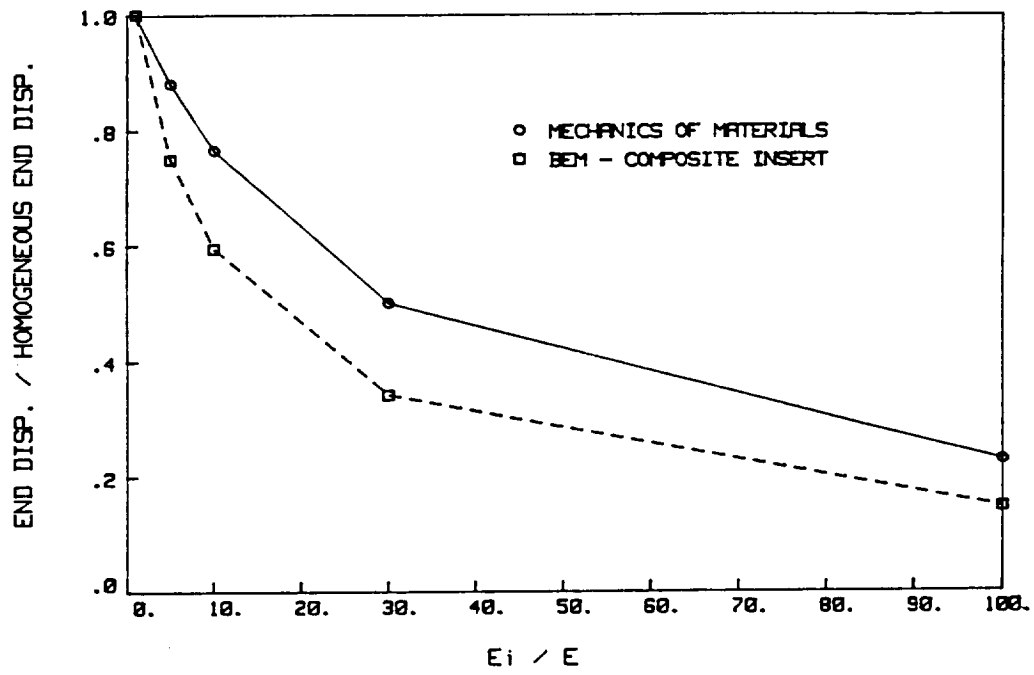


Fig. 6.6.2 Non-dimensionalized Vertical End Displacement of a Reinforced Beam in Bending vs. the Modulus of the Insert Over Modulus of the Beam

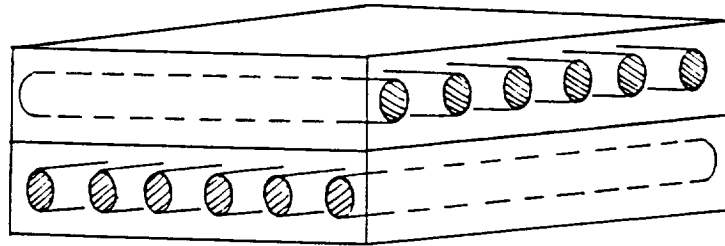


Fig. 6.7.1 Laminate-Fiber Composite

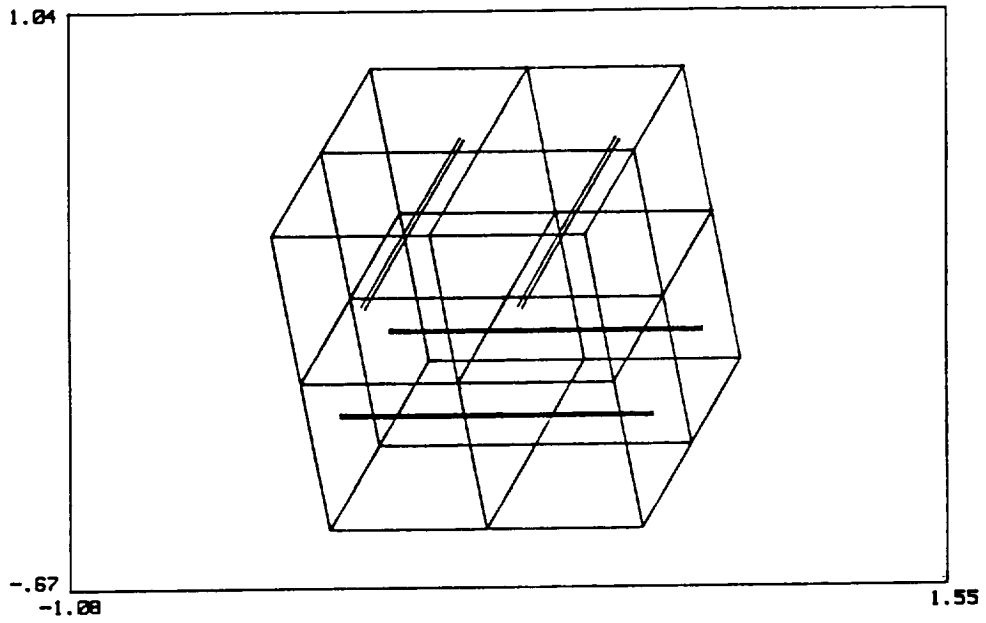


Fig. 6.7.2 BEM Discretization of a Laminate-Fiber Composite

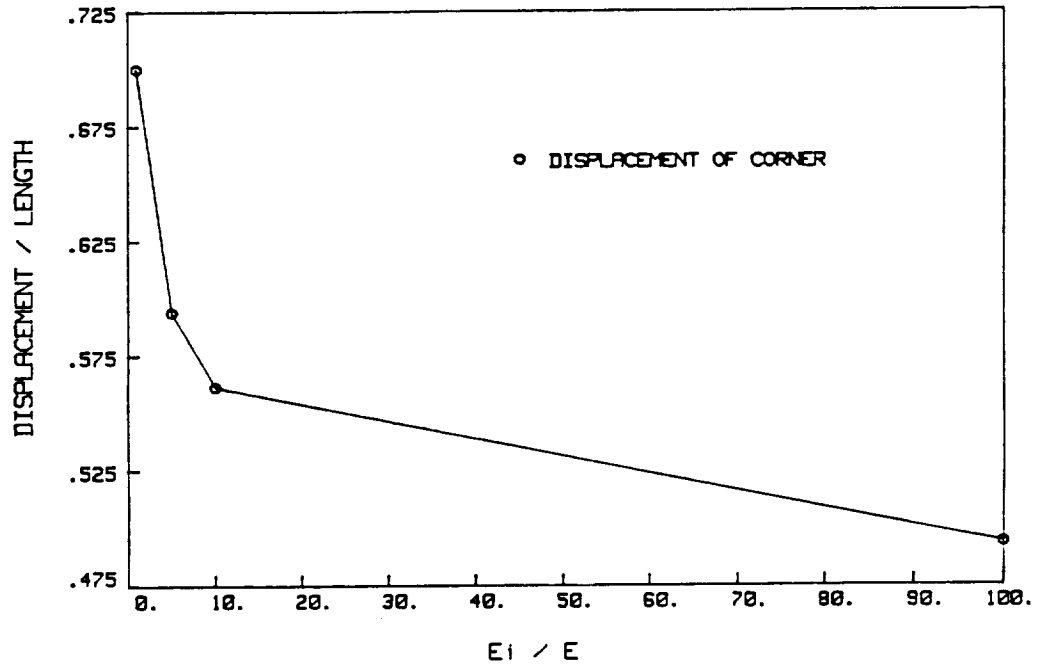


Fig. 6.7.3 Lateral Displacement of a Point at the Corner of the Interface of a Laminate-Fiber Composite Under Bi-axial Tension

7. SUMMARY OF CURRENT ACHIEVEMENT

As is evident from the previous section, significant progress has been made towards the goal of developing a general purpose boundary element program for the micromechanical studies of advanced ceramic composites. The formulation for elastostatic analysis of fully-bonded inserts has been implemented and validation runs have been shown to correlate with results obtained by full three-dimensional boundary element analyses. The composite insert code development is based on the advanced boundary element program BEST3D and all of its general purpose features have been retained in the new code. These facilities which include definition of local boundary conditions and multi-region substructuring will allow real problems encountered in industry to be analyzed.

Considerable effort has been focused in developing a formulation that is not only accurate, but computer efficient. For instance, analytical integration has been performed on the kernel function of the insert and hole in order to expedite numerical integration. Also a new boundary integral equation formulation was developed to both facilitate an efficient assembly scheme for the inserts, and to reduce the number of unknowns in the system and therefore render a smaller set of equations which is less expensive to solve.

Overall the cost of the new composite insert analysis is just slightly more expensive (for a moderate number of inserts) than the cost of analyzing the matrix without the inserts present. The additional cost is primarily attributed to the additional integration of the outer surface of the matrix which is required for additional nodes on the insert's hole, and towards the expense of solving a slightly larger system. In any case the price is far less than the cost required for a full three-dimensional, multi-region analysis of the same problem since in the 3-D approach more

two-dimensional surfaces must be integrated and far more additional equations (for the nodes describing the hole and the insert region) must be integrated and added to the equation system. The data preparation for the present method is far less involved than a full three-dimensional modeling of the composite insert using the ordinary multi-region approach. Furthermore, the code developed for the present work allows up to 500 (100 per GMR) insert elements in an analysis. An ordinary multi-region code would require a 500 region capability in order to compete. In terms of computer expense and the cost of data preparation for a 500 region problem, such analyses would be impractical.

The work in this initial year has demonstrated the accuracy and efficiency of the composite insert formulation applied to elastostatics. The method is not only perhaps the best tool, but also may be the only practical tool for the analysis of composite inserts in real problems encountered in industry. The boundary element method already has been proven successful in multi-region, transient and steady-state, elastodynamic and heat conduction analysis. Coupled with the success of the present work, the plan of this contract to extend the composite insert formulation in these other areas holds great potential.

8. FUTURE DEVELOPMENT

Significant progress has been achieved in the first year in developing a user friendly, ceramic composite base program. The infrastructure of the program is set up to facilitate future development. Presently the elastoplastic analysis for fully-bonded composite inserts has been implemented and tested. Delivery of the present code is planned for March 1989.

The remaining work on the present contract consists of: extending the formulation to steady-state and transient elastodynamic and heat transfer analysis; developing sophisticated interface connections including failure at the interface; and incorporating thermal and nonlinear material phenomena in the problem. The sequence for development of these tasks are inconsequential since they are relatively independent of one another. A workplan for their development is presented below, however, communication with interested parties at NASA will influence the exact order in which the work will be performed.

The primary thrust for the upcoming year will be directed toward the incorporation of more sophisticated interface conditions. Phenomena of interest include imperfect bonding, progressive debonding, cracking of the matrix, and controlled tension failure of the fibers. Initially this work will be developed for elastostatics, and extended to the other analysis types as they are developed.

Also during the next year, work will focus on the development of a ceramic composite analysis capability for steady-state heat conduction and the extension of thermal effects in elastostatics analysis. One-dimensional representations of fully-bonded ceramic fibers will be developed and incorporated into the code for heat conduction analysis, however, the suitability of the one-dimensional functional approximations

must be critically examined for geometrics and material properties typical of ceramic composites. In particular, it may prove necessary to employ a sine-cosine variation in the circumferential direction similar to the elastostatic formulation. Accuracy will be assessed via comparison with full three-dimensional BEST3D analyses. During the development for steady-state heat conduction and thermoelasticity, the thermal contact resistance between the matrix and insert interface will be added.

Presently the insert fibers are entered in the data input of the program as individual one-dimension line element with a prescribed radius. This provided tremendous advantages over the full 3D approach in terms of both modeling effort and computational efficiency. However, from a user's standpoint, even the one-dimensional representation is cumbersome if each fiber centerline must be defined. Clearly, a more convenient user interface is needed in order to provide a practical tool for micromechanical analyses of ceramic composites. This interface has been designed and will be implemented as part of the second year effort. As a result, the positioning of fibers will be determined internally by the program within any generic modeling region based upon the specification of a few keyword-driven parameters. With this approach, the user need only define the outer surface of the body, as in any typical BEST3D model, along with parameters specifying the overall fiber content, shape, size and orientation. Finally, an updated version of the ceramic composite code will then be made available at year end.

During the remaining three years, ceramic composite analysis capability will be developed for transient heat conduction, steady-state and transient elastodynamics, and material nonlinearities at high temperatures. The primary task will involve the development of appropriate representations for the inserts. Of course, now this task is much more

difficult due to the complexity of the governing differential equations and fundamental solutions. Additionally, investigations will be required to determine appropriate nonlinear material models and solution algorithms for the elevated temperature response of ceramic composites, and extensive testing of all of the capabilities will be conducted. Specific priorities for this advanced work will be established during 1989. Validation and verification runs will be conducted regularly, so that reliability is maintained throughout the duration of the five-year program. Once again, at the end of each program year, the resulting general purpose micromechanical ceramic composite code will be deliverable.

The final version, in particular, will provide a very precise, yet very efficient, user-friendly, design and analysis tool for ceramic composites exposed to severe operating environments. The resulting computer code will enable an engineer to undertake rapid numerical experiments to gain insight into the micromechanics of a particular composite. Armed with this information, the disposition of fibers can be selected to optimize performance under inelastic, thermal and dynamic loading.

LIST OF SYMBOLS

A^b, B^b	Boundary system matrices in assembled form
$C_{ij}(\xi)$	A tensor dependent on location of the field point ξ
G_{ij}, F_{ij}	Kernels of the displacement equation
$N^Y(\eta)$	One-dimensional shape function
$M^\beta(\eta_1, \eta_2)$	Two-dimensional shape function
t_i	Traction
u_i	Displacement
x	Refers to global coordinates of an integration point
\mathbf{x}	System vector of unknown boundary quantities
\mathbf{y}	System vector of known boundary quantities
ε_{ij}	Strain
η	Refers to local coordinate of an integration point
ν	Poisson's ratio
ξ	Refers to coordinates of a field point
σ_{ij}	Stress
Subscript	
$,$	Spatial derivative
i, j, k	Indicial notation
	$i, j, k = 1, 2, 3$

REFERENCES

- Banerjee, P.K., 'Integral Equation Methods for Analysis of Piece-wise Non-homogeneous Three-dimensional Elastic Solids of Arbitrary Shape', *Int. J. Mech. Sci.*, 18, pp. 293-303 (1976).
- Banerjee, P.K. and Butterfield, R., Boundary Element Methods in Engineering Science, McGraw-Hill, London (1981).
- Banerjee, P.K. and Butterfield, R., Developments in Boundary Element Methods - I, Applied Sci. Publishers, Barking, Essex, UK (1979).
- Banerjee, P.K. and Driscoll, R.M., 'Three-dimensional Analysis of Raked Pile Groups', *Proc. of Inst. Civil Engineers, Research and Theory*, Vol.61, pp. 653-671 (1976).
- Banerjee, P.K. and Mukherjee, S. Developments in Boundary Element Methods - III, Applied Sci. Publishers, Barking, Essex, UK (1984).
- Banerjee, P.K. and Shaw, R.P., Developments in Boundary Element Methods - II, Applied Sci. Publishers, Barking, Essex, UK (1982).
- Behrens, E., 'Thermal Conductivities of Composite Materials', *J. Composite Materials*, Vol. 2, p. 2 (1968).
- Butterfield, R. and Banerjee, P.K., 'Analysis of Axially Loaded Compressible Piles and Pile Groups', *Geotechnique*, Vol. 21, No. 1, pp. 43-60 (1971).
- Caruso, J.J. and Chamis, C.C., 'Assessment of Simplified Composite Micromechanics Using Three-dimensional Finite-Element Analysis', *J. Comp. Tech. Res.*, Vol. 8, No. 8, pp. 77-83 (1986).
- Chamis, C.C. and Sendekyj, G.P., 'Critique on Theories Predicting Thermoelastic Properties of Fibrous Composites', *J. Composite Materials*, Vol. 2, p. 332 (1968).
- Chamis, C.C. and Sinclair, J.H., 'The Effects of Eccentricities on Fracture of Off-axis Fiber Composites', *Polym. Eng. and Sci.*, Vol 19, No. 5 (April 1979).
- Cruse, T.A. and Wilson, R.B., 'Advanced Applications of Boundary-integral Equation Methods', *Nuc. Engng. and Des.*, 46, pp. 223-234 (1977).
- Cruse, T.A. and Wilson, R.B. 'Boundary-integral Equation Methods for Elastic Fracture Mechanics Analysis', AFOSR-TR-78-0355 (1978).
- Dongarra, J.J., et al, Linpac Users' Guide, SIAM, Philadelphia, PA (1979).
- Davidge, R.W., 'Fibre-reinforced Ceramics', *Composites*, Vol. 18, No. 2, pp. 92-97 (1987).
- Garg, K.S., Svalbonas, V. and Gurtman, G., Analysis of Structural Composite Materials, M. Decker, New York (1973).

Hashin, Z. and Rosen, B.W., 'The Elastic Moduli of Fiber Reinforced Materials', J. Appl. Mech., Vol. 31, p. 223 (1964).

Hill, R., 'Theory of Mechanical Properties of Fibre-strengthened Materials: III. Self-consistent Model', J. Mech. Phys. Solids, Vol. 13, p. 189 (1965).

Jones, R.M., Mechanics of Composite Materials, McGraw-Hill (1975).

Lachat, J.C. and Watson, J.O. 'Effective Numerical Treatment of Boundary Integral Equations: A Formulation for Three-dimensional Elastostatics', Int. J. Num. Meth. in Engrg., 10, pp. 991-1005 (1976).

McCullough, R.L., Concepts of Fiber-resin Composites, M. Decker, New York (1971).

Rizzo, F.J., 'An Integral Equation Approach to Boundary Value Problems of Classical Elastostatics,' Quart. Appl. Math., 25, No. 1, pp. 83-85 (1967).

Rizzo, F.J. and Shippy, D.J., 'A Formulation and Solution Procedure for the General Non-homogeneous Elastic Inclusion Problem', Int. J. Solids and Struct. 4, pp. 1161-1179 (1968).

Rizzo, R.R., 'More On the Influence of End Constraints on Off-axis Tensile Tests', J. Composite Materials, Vol. 3, p. 202 (1969)

Sen, R., Kausel, E. and Banerjee, P.K., 'Dynamic Behavior of Axially and Laterally Loaded Piles and Pile Groups Embedded in Inhomogeneous Soil', Int. Jour. Numerical Analytical Methods in Geomechanics, Vol. 9, No. 6, pp. 507-524, (1985).

Stroud, A.H. and Secrest, D., Gaussian Quadratic Formulas, Prentice Hall, New York (1966).

Vinson, J.R. and Chou, T.W., Composite Materials and Their Use in Structures, John Wiley and Sons (1975).

Watson, J.O., 'Advanced Implementation of the Boundary Element Method for Two- and Three-dimensional Elastostatics', in Banerjee, P.K. and Butterfield, R., Developments in Boundary Element Methods - I, Applied Science Publishers, London, pp. 31-64 (1979).

Whitney, J.M. and Riley, M.B., 'Elastic Properties of Fiber Reinforced Composite Materials', J. AIAA, Vol. 4, p. 1537 (1966).

Wilson, R.B., Bak, M.J., Nakazawa, S., and Banerjee, P.K. '3-D Inelastic Analysis Method for Hot Section Components (Base Program)', NASA Contract Report 174700 (February 1984).

